Talanta 211 (2020) 120700

Contents lists available at ScienceDirect

Talanta

journal homepage: www.elsevier.com/locate/talanta

Biosensors on the road to early diagnostic and surveillance of Alzheimer's disease

Pedro Carneiro[a,b], Simone Morais[b,*], Maria do Carmo Pereira[a]

[a] LEPABE - Laboratory for Process Engineering, Environment, Biotechnology and Energy, Faculty of Engineering, University of Porto, Rua Dr. Roberto Frias, 4200-465, Porto, Portugal

[b] REQUIMTE–LAQV, Instituto Superior de Engenharia do Porto, Instituto Politécnico do Porto, R. Dr. António Bernardino de Almeida 431, 4200-072, Porto, Portugal

ARTICLE INFO

Keywords:
Alzheimer's disease
Optical
Electrochemical
Biosensor
Nanomaterials

ABSTRACT

Alzheimer's disease is a debilitating and largely untreatable condition with subtle onset and slow progression over an extensive period of time, which culminate in increasing levels of disability. As Alzheimer's disease prevalence is expected to grow exponentially in the upcoming decades, there is an urgency to develop analytical technologies for the sensitive, reliable and cost-effective detection of Alzheimer's disease biomarkers. Biosensors are powerful analytical devices that translate events of biological recognition on physical or chemical transducers into electrical, thermal or optical signals. The high sensitivity and selectivity of biosensors associated with easy, rapid and low-cost determination of analytes have made this discipline one of the most intensively studied in the past decades.

This review centers on recent advances, challenges and trends of Alzheimer's disease biosensing particularly in the effort to combine the unique properties of nanomaterials with biorecognition elements. In the last decade, impressive progresses have been made towards the development of biosensors, mainly electrochemical and optical, for detection of Alzheimer's disease biomarkers in the pico- and femto-molar range. Nonetheless, advances in multiplexed detection, robustness, stability and specificity are still necessary to ensure an accurate and differentiated diagnosis of this disease.

1. Introduction

Alzheimer's disease (AD) is the most common human neurodegenerative disease (NDD) that commonly manifests itself in the form of dementia [1–3]. Its incidence increases with age and, like most NDDs, AD is considered a multifactorial condition mainly characterized

Abbreviations: AAO, Anodic aluminum oxide; ABTS, 2,2′-zinobis-(3-ethylbenzothiazoline-6-sulphonate); ABTS-PDDA/SWCNTs, 2,2′- azinobis-(3-ethylbenzothiazoline-6-sulphonate)-poly(diallyldimethylammonium chloride)-bi functionalized single-walled carbon nanotubes composite; aCSF, Artificial cerebrospinal fluid; AD, Alzheimer's disease; AgNPs, Silver nanoparticles; ALP, Alkaline phosphatase; APMES, 3-(ethoxydimethylsilyl) propylamine; ApoE, Apolipoprotein E; APP, Amyloid precursor protein; APTES, 3-aminopropyltriethoxysilane; APTMS, 3-aminopropyltrimethoxysilane; Arg, Arginine; AuE, Gold electrode; AuNPs, Gold nanoparticles; Aβ, Amyloid beta peptide; $BMIMBF_4$, 1-butyl-3-methyl-imidazolium tetrafluoroborate; CNTs, Carbon nanotubes; CS, Cysteamine; CSF, Cerebrospinal fluid; CV, Cyclic voltammetry; DDA, 4,4 -dithiodibutyric acid; DMF, N,N-dimethylformamide; DMSO, Dimethyl sulfoxide; Cys, Cysteine; DNA, Deoxyribonucleic acid; DPV, Differential pulse voltammetry; DTSP, Dithiobis (succinimidyl propionate); ECL, Electrochemiluminescence; EDC, 1-ethyl-3-(3-dimethylaminopropyl) carbodiimide; EDTA, Ethylenediamine tetraacetic acid; EIS, Electrochemical impedance spectroscopy; ELISA, Enzyme-linked immunosorbent assays; FITC, Fluorescein isothiocyanate; GCE, Glassy carbon electrode; GO, Graphene oxide; GOx, Glucose oxidase; HRP, Horseradish peroxidase; ITO, Indium tin oxide; LOD, Limit of detection; LSPR, Localized surface plasmon resonance; MES, 2-(N-Morpholino) ethanesulfonic acid; MHDA, 16-mercaptohexadecanoic acid; MNH, 9-mercapto-1-nonanol; MOFs, Metal organic frameworks; MPA, Mercaptopropionic acid; MU, 11-mercapto-1-undecanol; MUA, 11-mercaptoundecanoic acid; MUD, 11-mercaptoundecanol; MWCNTs, Multi-walled carbon nanotubes; NDDs, Neurodegenerative diseases; NHS, N-hydroxysuccinimide; NHSS, N-hydroxysulfosuccinimide; NKB, Neurokinin B; ODT, 1,8-octanedithiol; *p*-AP, *p*-aminophenol; p-APP, *p*-aminophenyl phosphate; PBS, Phosphate buffered saline; PDDA, poly(diallyldimethylammonium chloride); PEG, Polyethylene glycol; poly(DMA-co-NAS-co-MAPS), Ter-copolymer made with an optimised composition of dimethylacrylamide (DMA), 3-(trimethoxysilyl) propyl methacrylate (MAPS) and N-Acryloyloxy succinimide ester (NAS); POPA, Co-polymer of polytyr-amine/3-(4-hydroxyphenyl) propionic acid; p-Tau, Phosphorylated tau; QCM, Quartz crystal balance; QD, Quantum dots; SA-ALP, Streptavidin-modified alkaline phosphatase; SAM, Self-assembled monolayer; SF, Silk fibroin; SPCE, Screen-printed carbon electrode; SPGE, Screen-printed gold electrode; SPR, Surface plasmon resonance; STM, Scanning tunneling microscopy; SWV, Square-wave voltammetry; t-Aβ, Total Aβ; TCEP, Tris(2-carboxyethyl)phosphine; t-Tau, Total tau; ZIF-8, Zeolitic imidazole framework

* Corresponding author.
E-mail address: sbm@isep.ipp.pt (S. Morais).

https://doi.org/10.1016/j.talanta.2019.120700
Received 11 October 2019; Received in revised form 21 December 2019; Accepted 28 December 2019
Available online 03 January 2020
0039-9140/

by the aggregation of a small number of proteins [1–3]. Approximately 40 million people, mostly older than 60 years, have dementia and this number is expected to triple by 2050, being recognized by the World Health Organization as a global public health priority [2,4–8]. Therefore, it is of the utmost importance to develop analytical tools that can contribute to the identification and determination of biomarkers for AD in order to facilitate the diagnostic process and identification of patients at earlier stages, as well as monitor biochemical effects of treatments. Moreover, with the implementation of new and more efficient diagnostic techniques, it will be possible to provide patients a healthier and more reliable life by slowing or preventing the disease progression in its early stages [5].

The present review focuses on the advances made in the last decade (2008–2018) on the development and application of biosensors for detection of AD main biomarkers in artificial and real samples. In addition, it endeavors to explain how nanomaterials are used to improve the biosensors performance highlighting their interaction with the biorecognition elements focusing on several techniques used to promote their immobilization. Finally, it brings into focus future perspectives on the biosensing of AD.

The available scientific literature, in the period between 2008 and 2018, was searched in the Thomson Reuters ISI Web of Knowledge, Science Direct, PubMed and Google Scholar databases by combining at least two of the following keywords: biosensor/electrochemical immunosensor/optical biosensor/surface plasmon resonance and Alzheimer's disease/Amyloid beta/Tau protein/Apolipoprotein E.

2. Alzheimer's disease

AD is the most common cause of dementia with severe impacts on individuals and society [2,9–12]. Research, in recent decades, has culminated in the evidence that the formation of extracellular amyloid beta (Aβ) plaques and intracellular neurofibrillary tangles of hyperphosphorylated tau protein are the main causes for the development of AD [2,6,9,13–15]. Moreover, these two processes are usually accompanied by neuroinflammation and oxidative stress, all of which contribute to the loss of synaptic integrity and neural network connectivity [2,6,9,14,16,17]. Amyloid plaques are extracellular accumulations of abnormally folded Aβ peptides, Aβ40 (40 amino acids) and Aβ42 (42 amino acids), derived from proteolytic cleavage of the glycoprotein amyloid precursor protein (APP) by β- and γ-secretase activities, being the variant with 42 amino acids more prone to aggregate [2,6,12,14–16]. Research gives support to the fact that the primary event in AD may result from an imbalance between the production and clearance of Aβ in the brain, leading to the overexpression of Aβ42 and consequent aggregation, from which all other stages of the disease unfold [12,18]. Although the formation of amyloid plaques composed of Aβ aggregates has been thought for decades to be the critical pathological hallmark of AD, a lot of evidence has brought to light that Aβ oligomers may be its most pathological form [12,19]. The fact that one-third of the elderly die with evidence of Aβ accumulation without noticeable symptoms proves that while remaining essential for AD diagnosis Aβ deposition on its own is not enough to cause dementia in AD [8,12,20].

Neurofibrillary tangles made of intracellular aggregations of paired helical filaments of abnormal phosphorylated tau protein, have also been investigated as a biomarker [2,12,21–24]. Tau in AD undergoes abnormal phosphorylation becoming unable to bind and stabilize microtubules, leading to protein misfolding and subsequent aggregation as neuropil threads in dystrophic neurites and as neurofibrillary tangles which, eventually, results in loss or decline of axonal or dendritic transport [22–24]. Tau protein undergoes several modifications being phosphorylation on multiples sites considered to be a major early event in the formation of tau inclusions [25]. To get a comprehensive overview of these post-translational modifications, several modified sites have to be assessed at a qualitative and quantitative level which can be extremely challenging due to the large number of modified sites and existence of multiple types of modifications [25]. Current strategies struggle to distinguish these post-translational modifications of tau protein mainly associated with epitopes variability which affects the affinity of the biological recognition elements that in turn disturbs the rigorous quantification of tau protein [25].

The identification of mutations in gene coding for proteins involved in Aβ deposition/clearance pathways, as the case of apolipoprotein E (ApoE), constitutes another pathological hallmark of the disease. ApoE is a 299 amino acid protein produced primarily by astrocytes and microglia with three common isoforms in humans (ApoE2, ApoE3 and ApoE4) that only differ by 1 or 2 amino acids impacting the charge and structural properties of the protein and, ultimately, their functional properties [9,26–29]. Studies have revealed that deposition of Aβ into plaques can be influenced by isoforms and amount of ApoE present in the central nervous system, inevitably impacting the onset and progression of AD [27]. This way, ApoE4 increases the risk of developing AD and it is also associated with earlier onset of the disease [9,26,27,29]. On the other hand, ApoE2 reduces the risk of developing AD by decreasing the deposition of Aβ and delaying the onset time [9,27,29].

Increasingly, AD is being classified as a multifactorial disorder that arises from the interaction of multiple pathogenic factors, such as amyloid precursor protein, Aβ, Tau protein, ApoE and other co-morbidities.

Currently, the field of drug development concerning AD is directing its efforts towards the development of disease-modifying drugs being these treatments more likely to succeed when administrated in the early stages of disease. Therefore, the development of diagnostic tools capable of performing an early, accurate and differential diagnosis is of vital importance [30]. However, several clinical and neuropathological studies have classified the criteria for AD diagnosis to be suboptimal as this process is mostly based on clinical assessment of symptoms, which can lead to misdiagnosis or diagnosis made in advanced stages of the pathology, which in turn can influence the course of several drug candidates when tested in clinical trials [5,30]. Biomarkers such as Aβ and tau protein can have a pivotal role in developing more accurate diagnosis tools for AD and their use was recommended in recent research diagnostic guidelines for AD by the National Institute on Aging–Alzheimer's Association [30,31] and International Work Group 2 criteria [30,32]. To date, the only biomarker that has been approved by the Food and Drug Administration was the evaluation of Aβ through positron emission tomography scans providing a visual aid to assess the presence of Aβ plaques [30]. On the other hand, this is an expensive and specialized procedure with radioactive burden on the patient. Therefore, cerebrospinal fluid (CSF) biomarkers appear as a viable alternative as several studies have shown unequivocally that AD is associated with lower CSF levels of Aβ42 and higher CSF levels of total tau (t-tau) and phosphorylated (p-tau) being able to distinguish patients with AD *versus* controls, also in the early stages [8,33,34]. In addition, the evaluation of the ratio Aβ42/Aβ40 has proven to increase diagnostic accuracy [35].

3. Alzheimer's disease biosensors

3.1. Generic overview

A biosensor is defined by the International Union of Pure and Applied Chemistry as an integrated receptor-transducer device capable of providing specific quantitative or semi-quantitative analytical information using a biological recognition element [36–39]. Biosensors can be classified in terms of the bioreceptor, type of transducer used or both [39]. The bioreceptor is the molecular species responsible for detection and identification of the chemical or biological analyte in order to perform a selective and accurate diagnosis thus becoming the key component of a biosensor [40,41]. Based on the type of

biorecognition element, biosensors can be classified as immunosensors (antibody-antigen), nucleic acid, cell/tissue and enzymatic biosensors, which can be further divided in two broad categories according to the biorecognition principle [39,40,42,43]. Catalytic biosensors are typically characterized by the use of enzymes for the biological recognition events while affinity biosensors, termed as a result of the high affinity of biological events and species used for biorecognition, englobe the use of antibodies and DNA [43]. In addition, biosensors can be further categorized as optical, thermal, piezoelectric and electrochemical, depending on the type of signal [39,40,44,45]. Concluding, biosensors are devices capable of converting biological activity into a measurable electronic signal, which can be detected through several techniques each having its own strengths and weaknesses. The relatively low cost, rapid response and possibility of miniaturization of biosensors make them useful in a variety of fields including healthcare, biological analysis, environmental monitoring and food quality control, among others [38,46–48].

The electrode material and fabrication specifications are crucial aspects of the development of a biosensor as they will directly impact the device performance, particularly the manner in which the electrodes surface is going to be modified and coated [43,46,49,50]. Screen-printed electrodes (SPEs) have been receiving a lot of attention in recent years with applications in a wide range of fields due to their operation simplicity, reliability, potential portability and small instrumental setups as they comprise the working, reference and auxiliary electrodes in the same low-size platform [43,50–54]. In addition, the disposable feature of SPEs make them reliable platforms for the direct analysis of several samples of different origins preventing electrode poisoning from recurrent use [52–54].

The stimulating breakthroughs observed in the past decades in the development and synthesis of nanomaterials had a tremendous impact in the growth of biosensing technology as nanomaterials with different sizes, shapes and unique physical and chemical properties have been showing a crucial role in designing highly sensitive and selective biosensors [47,51,55–61]. As a result of their quantum-size effects, nanostructured materials have been applied in very different ways as they can improve the conductivity or catalytic activity of a transducer while their high surface-to-volume ratio and large surface areas make them excellent matrices for the immobilization of biorecognition elements improving the overall performance and sensitivity of a biosensor [51,55–62].

One of the key parameters to ensure long-term operational stability of a biosensor is the appropriate immobilization of biomolecules on the surface of nanomaterials, i.e. an immobilization that retains the full biological activity of the biorecognition element while providing an effective electronic connection between the redox-active sites in the biomolecule and the electrode surface [39,43,48,56,63–69]. Thus, intense research has been focused on the selection of the best techniques to promote immobilization of biomolecules with proper orientation [59,65–67,69]. Immobilization of biological components on the surface of transducers can involve varying levels of difficulty from simple and nonspecific methods, which often results in randomly oriented proteins, to highly structured bioconjugates with oriented immobilization, higher stability and reproducibility [66]. The simplest methods that have been used are based on physical immobilization, which can be promoted mainly via electrostatic force, ionic bonds and hydrophobic interactions [59,65–67]. In addition, entrapment in (bio)polymer matrices has also been used to promote better attachment of biomolecules [66,67]. Nonetheless, physical immobilization often results in random orientation and weak attachment and even in the cases of entrapment, limited recognition efficiency is still a problem due to burying of recognition sites [67]. A more robust, stable and reproducible way to immobilize bioreceptors, that results in higher sensitivity, is through covalent bonding involving the coupling of reactive chemical groups present on the protein and on the transducer surface [65–67]. Covalent links can be formed by amine, carboxyl and thiol coupling reactions, cross-linking reagents, such as glutaraldehyde, thiol derivatives and polymers, or click chemistry [59,65–67]. Despite its crucial role in protein immobilization, covalent bonding has still one major drawback related with uncontrolled anchoring of biomolecules, which inevitably affects the domain responsible for the recognition event [67]. This way, techniques that promote site specific immobilization have also been explored. Non-covalent approaches for site-specific immobilization are based on bioaffinity interactions. The most widely applied is the biotin-strept(avidin) interaction where biotinylated biomolecules can be attached to substrates via avidin (or streptavidin) bridges [59,67]. Another commonly used affinity based immobilization tag is through binding of biorecognition elements to protein G or A. Site-specific immobilization can also be achieved via covalent bonding through the introduction of unique chemical groups or sequences, such as azides or alkynes, at a specific location that will covalently bind the protein to the complementary functionalized surface, without affecting the binding domain [59,67,69]. In addition, there is still the possibility of protein engineering, as for example through cleavage of the antibody at the hinge region in order to take advantage of their native thiol groups for immobilization on gold surfaces [64,67,68].

3.2. Applications of Alzheimer's disease biosensors

Over the last decade, AD has been the most intensively studied neurodegenerative disease with regard to biomarkers detection, in blood and CSF, of mainly Aβ [70–93], tau protein [94–104], ApoE [105–111] and multiple detection of these same biomarkers [112–121]. While the roles of Aβ and Tau protein in AD are well described in literature [2,8,9], ApoE, and particularly the isoform ApoE4, has been receiving a lot of attention as a major genetic risk for AD as it can predict accumulation of Aβ in the brain [2,9,27,28]. Configuration, analytical performance and application of the biosensors developed in the last decade for AD biomarkers are displayed in Tables 1–4. Table 1 characterizes the biosensors for Aβ biomarker and related variants [70–93]; Table 2 focuses on the biosensors for tau protein determination [94–104]; Table 3 exhibits the biosensors for ApoE detection [105–111] and Table 4 shows the biosensors capable of performing multiple determination of the aforementioned biomarkers [112–121].

Electrochemical immunosensors are the most reported for determination of the selected biomarkers as they combine the high sensitivity displayed by electroanalytical methods with the inherent specificity associated with biological recognition events, in this case the high affinity achieved through antibody-antigen interactions. In addition, the operational simplicity, low-cost of instrumentation, inherent miniaturization and potential of automation related to electrochemical immunosensors make them excellent instruments for determination of trace amounts of biological agents. The most common transducers used throughout the reviewed studies (Tables 1–4) were glassy carbon (GCE) [73,79,106,114] (Tables 1, 3 and 4), gold (AuE) [78,90–93,95–98,112,113] (Tables 1, 2 and 4), indium tin oxide (ITO) [87,108–111] (Tables 1 and 3) and carbon screen-printed electrodes (SPCE) [74–76,99,105,120] (Tables 1–4). Nevertheless, other materials such as anodic aluminum oxide membrane (AAO) [77] (Table 1), silicon wafer [80,81,83] (Table 1) and gold screen-printed electrodes (SPGE) [88] (Table 1) were also used.

In recent decades nanomaterials have become an integral part of almost every biosensor development. This way, the transducers used in the reviewed studies were commonly modified with various nanomaterials such as gold (AuNPs) [74–79,82–84,87,98,110–112,114,119,120] (Tables 1–4), silver (AgNPs) [118] (Table 4) and silica nanoparticles [100] (Table 2), magnetic beads/spheres [105,107,120] (Tables 3 and 4), polymers [71,72,81,87,88,91,117,119] (Tables 1 and 4) and carbon nanomaterials such as graphene oxide (GO) [99,106,109] (Tables 2 and 3) and carbon nanotubes (CNTs) [70,73,103,114] (Tables 1, 2 and 4) but other nanomaterials, such as dendrimers [99] (Table 2) and quantum dots (QDs) [107,109] (Table 3)

Table 1
Configuration, analytical performance and application of the developed biosensors for Aβ biomarker and related variants determination.

Biomarker	Transducer	Detection Method	Sample	**Detection range (nM[a])**	**LOD (nM[a])**	References
Aβ42	CNTs-Metal semiconductor field effect transistor structure modified with *E. coli* outer membrane with autodisplayed Z-domains and immobilized antibodies	Electrical conductance	Human Serum	2.2×10^{-4} – 0.2215[a]	2.2×10^{-4}[a]	[70]
Aβ42	Interdigitated microelectrode with SiO_2 surface functionalized with APMES, polyvinyl pyrrolidone-aldehyde solution, sodium borohydride, glutaraldehyde and antibodies	Ion concentration polarization-based preconcentration - Measurement of impedance	Buffer	2.2×10^{-6} – 0.221[a]	8.15×10^{-6}	[71]
Aβ42	Interdigitated microelectrode with a SiO_2 layer which was later treated with APMES, polyvinyl pyrrolidone-aldehyde solution, sodium borohydride, glutaraldehyde and antibodies	Measurement of impedance	Buffer and mouse plasma	2.2×10^{-5} – 0.022[a]	–	[72]
Cu^{2+}; Aβ42	GCE functionalized with ABTS-PDDA/SWCNTs combined with neurokinin B	DPV	Buffer, Blood and Hippocampus of rats	Cu^{2+}) 100–10000 Aβ42) 0.22–8.42[a] 2.2–84.2[a] 22–842[a]	Cu^{2+}) 40 Aβ42) 0.11[a]	[73]
Aβ42	SPCE functionalized with AuNPs/mixed monolayers of PEG-SH and MPA and antibodies	Sandwich assay with ALP tagged antibody for DPV signal amplification	Buffer, Diluted human serum and Plasma	1×10^{-4} – 0.025	1×10^{-4}	[74]
Aβ42	SPCE modified with AuNPs and conjugate streptavidin-biotin to promote Aβ42 immobilization on the surface. Recognition antibodies and ALP labeled detection antibodies were used to perform the immunoassay. Biotin-Aβ42 and Aβ42 compete for the recognition antibody	Competitive immunoassay using anodic stripping of enzymatically generated silver by CV	Buffer	0.11–110.8[a]	0.022[a]	[75]
Aβ42	Carbon disposable electrochemical printed chip modified with AuNPs/MHDA SAM, Protein G and antibodies	EIS	Buffer	0.01–10	0.57	[76]
Aβ42	AAO substrate sputtered with a thin gold film functionalized with AuNPs, MUA and antibody immobilization through EDC/NHS interaction	EIS	Buffer	2.2×10^{-4} – 2.2[a]	2.2×10^{-6}[a]	[77]
Aβ42	AuE modified with a MPA SAM, AuNPs and chemically modified antibodies	SWV	Buffer	2.2×10^{-3} – 0.022[a]	1.15×10^{-3}[a]	[78]
Aβ42	GCE modified with $Ru(bpy)_3^{2+}$ caged in a 3D zinc oxalate MOFs and antibodies	Sandwich assay using antibodies conjugated with AuNPs and NiFe based nanocube MOFs - ECL	Buffer and aCSF	2.2×10^{-5} – 11.1[a]	3.0×10^{-6}[a]	[79]
Aβ42	Silicon wafer treated through silanization with carboxylated alkyltrichlorosilane modified with antibodies through EDC/NHS interaction	Immunoassay using a recognition and Cy5 labeled detection antibody - Fluorescent detection	Buffer-Tween	550–1660[a]	66[a]	[80]
Aβ42	Silicon microarray platform coated with poly(DMA-co-NAS-co-MAPS) modified with antibodies	Biotin-labeled secondary antibody and Cyanine 3 labeled with streptavidin - Fluorescent detection	aCSF	0.022–1.1[a]	0.016[a]	[81]
Aβ42	AuNPs functionalized with antibodies against Aβ42	Colorimetric sandwich immunosensor	Buffer and Serum samples	7.5–350	2.3	[82]
Aβ42	Sputtered gold on a silicon wafer that was later modified with ODT SAM and antibody fragments	Sandwich Immunoassay using AuNPs functionalized with antibodies - STM detection	Buffer	2.2×10^{-6} – 220[a]	2.2×10^{-6}[a]	[83]
Aβ42	Glass slides treated with APTES and absolute ethanol and modified with AuNPs modified with Aβ42 and ApoE4 as chaperone	LSPR	CSF buffer	1×10^{-3} – 10^{6}	1.5×10^{-3}	[84]
Aβ42	Waveguide-coupled bimetallic chip modified with a chloroform SAM and antibodies immobilized via a covalent bond through EDC/NHS	SPR	Buffer	0.022–0.44[a]	0.048[a]	[85]
Aβ40	Interdigitated AuE modified with DTSP SAM and antibodies	EIS	Buffer	0.01–100	0.01	[86]
Aβ40	ITO coated glass substrates modified with AuNPs and PEG	SWV	Buffer and Brain samples	100–500	4.78	[87]
Aβ oligomers	SPGE modified with biotinylated PrP^C (95–110) peptide tethered via biotin-NeutrAvidin in POPA co-polymer	EIS	DMSO/F12 medium and Chinese hamster ovary cell line	10^{-3} – 1000	5×10^{-4}	[88]
Aβ oligomers	Curcumin-Ni was electropolymerized on Ni foam substrate	EIS	Buffer and aCSF	0.001–5	1.0×10^{-3}	[89]
Aβ oligomers	AuE modified with cysteine- PrP (95–110). MU was used to block the unreacted gold surface	Sandwich assay using ALP- PrP(95–110) with CV detection	Buffer and Serum samples	5×10^{-3} – 2	3×10^{-3}	[90]
Aβ oligomers	AuE modified with Poly (pyrrole-2-carboxylic acid) linking agent and PrP^C receptor	EIS	Buffer and Brain samples	10^{-7} – 10	10^{-7}	[91]

(*continued on next page*)

Table 1 (*continued*)

Biomarker	Transducer	Detection Method	Sample	Detection range (nM[a])	LOD (nM[a])	References
Aβ42 oligomer	AuE modified with peptide probe (MUA – Ferrocene, I10 peptide), TCEP and MNH	SWV	Buffer and Serum samples	0.48–12	0.24	[92]
Aβ42 oligomer	AuE modified with assembly solution (protein binding peptide and TCEP) and MNH	SWV	Buffer	0.5–2.5	0.048	[93]

AAO, Anodic aluminum oxide; ABTS-PDDA/SWCNTs, 2,2′- azinobis-(3-ethylbenzothiazoline-6-sulphonate)-poly(diallyldimethylammonium chloride)-bi functionalized single-walled carbon nanotubes composite; aCSF, Artificial cerebrospinal fluid; ALP, Alkaline phosphatase; APMES, 3-(ethoxydimethylsilyl) propylamine; APTES, 3-aminopropyltriethoxysilane; AuE, Gold electrode; AuNPs, Gold nanoparticles; CNTs, Carbon nanotubes; CSF, Cerebrospinal fluid; CV, Cyclic voltammetry; DMSO, Dimethyl sulfoxide; DPV, Differential pulse voltammetry; DTSP, Dithiobis (succinimidyl propionate); ECL, Electrochemiluminescence; EDC, 1-ethyl-3-(3-dimethylaminopropyl) carbodiimide; EIS, Electrochemical impedance spectroscopy; GCE, Glassy carbon electrode; ITO, Indium tin oxide; LSPR, Localized surface plasmon resonance; MHDA, 16-mercaptohexadecanoic acid; MNH, 9-mercapto-1-nonanol; MOFs, Metal-organic frameworks; MPA, Mercaptopropionic acid; MU, 11-mercapto-1-undecanol; MUA, 11-mercaptoundecanoic acid; NHS, N-hydroxysuccinimide; ODT, 1,8-octanedithiol; PEG, Polyethylene glycol; poly(DMA-co-NAS-co-MAPS), Ter-copolymer made with an optimised composition of dimethylacrylamide (DMA), 3-(trimethoxysilyl)propyl methacrylate (MAPS) and N-Acryloyloxy succinimide ester (NAS); POPA, Co-polymer of polytyr-amine/3-(4-hydroxyphenyl) propionic acid; SAM, Self-assembled monolayer; SPCE, Screen-printed carbon electrode; SPGE, Screen-printed gold electrode; SPR, Surface plasmon resonance; STM, Scanning tunneling microscopy; SWV, Square-wave voltammetry; TCEP, Tris(2-carboxyethyl)phosphine.

[a] Value was expressed in μg mL^{-1}/ng mL^{-1}/pg mL^{-1} and converted to nM.

have also been used but to a lesser extent.

Gold nanoparticles were the most applied nanomaterials as they exhibit excellent electronic and optical properties in combination with good biological compatibility, ease of functionalization, controllable morphology and size, chemical stability, large surface area and high surface-to-volume ratio [47,66,122]. Carbon nanomaterials such as GO and CNTs have also been commonly applied in the development of electrochemical and optical biosensors. GO is a planar sheet of carbon atoms displaying large surface area, high mechanical strength, high electrical and thermal conductivity and high elasticity [123–125]. In addition, GO is also characterized by the presence of various oxygen functional groups [126]. On the other hand, CNTs are cylindrical molecules that consist of rolled-up sheets of single-layer carbon atoms that can be classified as single walled (SWCNTs) or multi-walled (MWCNTs) being characterized by their high surface-to-volume ratio, exceptional electronic properties, presence of edge-plane-like defects and ease of functionalization, all which contribute for the development of high performance biosensors [66,127,128]. At last, other type of nanomaterials that has been extensively applied for the development of biosensors were polymers mainly due to their ease of functionalization and high stability [47]. In addition, some polymers such as polypyrrole which are classified as conducting polymers also exhibit inherent electrical conductivity which can be highly relevant for electrochemical biosensors [47,129,130].

Another crucial parameter that requires extensive focus and optimization is related to the immobilization of the biological recognition elements. This way, different methods were applied to successfully immobilize the required biorecognition elements. Random physical adsorption has been one of the most commonly applied methods for antibody immobilization [70,82,86,90,103,105,107,108,110,131] (Tables 1–3). Nonetheless, the most common method to promote immobilization of biological recognition elements on AD biosensors was based on covalent bonding through EDC/NHS coupling [74,77,79,80,85,91,95,97–99,101,102,104,106,109,111–115,119,120] (Tables 1–4). Other methods such as conjugations through thiol groups [78,83] (Table 1), glutaraldehyde [71,72,99] (Tables 1 and 2) or polymers [81] (Table 1) have also been used. Despite being widely applied for immobilization of the biological recognition elements, the aforementioned methods face a big problem with uncontrolled anchoring of the biorecognition elements which can affect the function of their active sites. This way, to overcome this problem some works applied an affinity based method through the biotin-strept(avidin) interaction where biotinylated biomolecules can be attached to substrates via avidin (or streptavidin) bridges [59,67,75,88,117] (Tables 1 and 4). Another commonly used affinity based immobilization tag was through binding of antibodies to protein G [76,96,100] (Tables 1 and 2).

Different detection schemes and techniques were applied for detection of the main AD biomarkers mostly based on electrochemical and optical techniques. The main electrochemical techniques used throughout the reviewed works were square-wave voltammetry (SWV) [78,87,92,93,115] (Tables 1 and 4), differential pulse voltammetry (DPV) [73,74,98,99,106,109,114] (Tables 1–4) and electrochemical impedance spectroscopy (EIS) [76,77,86,88,89,91,94–97,110]. The remaining studies were mainly distributed between optical techniques, which relied on surface plasmon resonance (SPR) (Tables 1–4) [85,101–103,117] and localized surface plasmon resonance (LSPR) (Tables 1–4) [84,100,110,119], fluorescent detection (Tables 1, 3 and 4) [80,81,109,121], colorimetric methods (Tables 1, 3 and 4) [82,111,118] and microscopic techniques such as scanning tunneling microscopy (STM) (Table 1) [83].

Throughout this review, the studies that presented the best analytical behavior and lowest LODs were highlighted focusing particularly in those that were able to detect levels lower than the cut-off values in CSF of the main AD biomarkers.

Table 2
Configuration, analytical performance and application of the developed biosensors for Tau protein determination.

Biomarker	Transducer	Detection Method	Sample	**Detection Range (nM)**	**LOD (nM)**	References
Tau protein	384-multiwell microelectrode array coated with laminin	EIS	Cell culture medium	1–100	–	[94]
Tau protein	AuE functionalized with lipoic acid and NHS for tau protein immobilization with subsequent blocking with ethanolamine and backfilling with hexanethiol	EIS through analysis of tau-tau binding	MES + NaCl + EDTA	200–1000	200	[95]
Tau protein	Microband AuE covered with a layer of DTSSP SAM, protein G and antibodies	EIS	Buffer and Human serum	1×10^{-5} – 0.01	3×10^{-5}	[96]
Tau protein	AuE functionalized with antibodies through NHS coupling	EIS	Buffer	–	1100[a]	[97]
Tau protein-381	AuE modified with MPA SAM and antibodies	Sandwich immunoassay with aptamer–CS–AuNPs conjugate - DPV	Buffer and Human serum	5×10^{-4} – 0.1	4.2×10^{-4}	[98]
Tau protein	SPCE with graphene oxide and amine functionalized 1st generation trimethylolpropane tris[poly(propyleneglycol)] (pPG) dendrimers and antibodies for simultaneous detection of Myelin Basic and Tau proteins	Sandwich immunoassay with antibody conjugated carboxyl functionalized 3.5th generation pPG/CdS and pPG/PbS probes - DPV	CSF and Serum from Multiple Sclerosis patients	0.25–250	0.15	[99]
Tau protein	Chromium and gold deposited on glass slides that were functionalized with a DDA SAM, amino-surface-modified silica nanoparticles, gold layer, protein G and antibodies	LSPR	Buffer	1.7×10^{-4} – 1.7[a]	1.7×10^{-4}[a]	[100]
t-Tau p-Tau	AuE modified with MUA SAM and antibodies	SPR	Buffer and Human serum	t-Tau) 2.2×10^{-4} – 0.051[a] p-Tau) 8.18×10^{-3} – 3.57[a]	t-Tau) 5.3×10^{-7}[a] p-Tau) 1.3×10^{-3}[a]	[101]
Tau Protein-381	Gold chip functionalized with mixed SAMs of MUA and MUD and DNA aptamer probes	Sandwich assay using antibodies for Tau protein – SPR	Plasma	–	1×10^{-5}	[102]
Tau protein	Prism coupler modified with gold and antibodies	Sandwich immunoassay with antibodies coupled with MWCNTs - SPR	aCSF	0.125–1	0.125	[103]
Tau protein	Gold surfaces modified with a MU SAM and antibodies	1) Direct and 2) sandwich immunoassays: 2.1) antibody and 2.2) tubulin - QCM	aCSF	1) 0–250 2.1) 0–250 2.2) 0–500	1) 42 2.1) 10 2.2) 10	[104]

aCSF, Artificial cerebrospinal fluid; AuE, Gold electrode; AuNPs, Gold nanoparticles; CS, Cysteamine; CSF, Cerebrospinal fluid; DDA, 4,4 -dithiodibutyric acid; DPV, Differential pulse voltammetry; DTSSP, 3,3′-dithiobis (sulfosuccinimidyl propionate); EDTA, Ethylenediamine tetraacetic acid; EIS, Electrochemical impedance spectroscopy; LSPR, Localized surface plasmon resonance; MES, 2-(N-Morpholino) ethanesulfonic acid; MU, 11-mercapto-1-undecanoic acid; MUA, 11-mercaptoundecanoic acid; MUD, 11-mercaptoundecanol; MWCNTs, Multi-walled carbon nanotubes; NHS, N-hydroxysuccinimide; p-Tau, Phosphorylated tau; QCM, Quartz crystal balance; SPCE, Screen-printed carbon electrode; SPR, Surface plasmon resonance; t-Tau, Total tau.

[a] Value was expressed in $\mu g\ mL^{-1}$/$ng\ mL^{-1}$/$pg\ mL^{-1}$ and converted to nM.

Table 3
Configuration, analytical performance and application of the developed biosensors for ApoE determination.

Biomarker	Transducer	Detection Method	Sample	Detection Range (nM)	LOD (nM)	References
ApoE	SPCE modified with magnetic beads functionalized with antibodies	Sandwich immunoassay through iridium oxide nanoparticles with secondary antibodies - Chronoamperometry	Buffer and Human plasma	2.9–29.4[a]	2[a]	[105]
ApoE DNA	GCE modified with graphene-mesoporous silica hybrids coupled with methylene blue, ferrocenecarboxilic and DNA probe	DPV ratiometric signal detecting target DNA	Buffer	1×10^{-5} – 10	1×10^{-5}	[106]
ApoE	Graphite ink (microfluidic platform) modified with magnetic beads functionalized with antibodies	Sandwich immunoassay with biotinylated antibodies and streptavidin/QD conjugate - Square Wave Anodic Stripping Voltammetry	Buffer and Diluted human plasma	0.29–5.9[a]	0.37[a]	[107]
ApoE4	ITO electrode modified with polyelectrolytes, electrodeposited fractal gold nanostructures and antibodies	Sandwich immunoassay with HRP-labeled antibodies - Chronoamperometry	Buffer	0.029–290[a]	8.8×10^{-3}[a]	[108]
ApoE4 DNA	ITO modified with graphene-QD conjugates, electropolymerized curcumin and DNA probe	DPV and Fluorescence detection	Buffer and Human blood plasma	DPV) 20–400[b] Fluorescence detection) 45–400[b]	DPV) 2.18[b] Fluorescence detection) 12.4[b]	[109]
ApoE DNA	ITO modified with AuNPs and oligonucleotides	LSPR and EIS	Buffer	–	LSPR) 512 EIS) 286	[110]
ApoE	ITO modified with APTMS, glutaraldehyde, ionic liquid ($BMIMBF_4$)-chitosan, AuNPs and antibodies	Sandwich assay using Au–TiO_2, GOx, and anti-ApoE – Colorimetric detection using glucose	Buffer and Serum	2.9×10^{-5} – 0.290[a]	1.2×10^{-5}[a]	[111]

APTMS, 3-aminopropyltrimethoxysilane; AuNPs, Gold nanoparticles; $BMIMBF_4$, 1-butyl-3-methyl-imidazolium tetrafluoroborate; DNA, Deoxyribonucleic acid; DPV, Differential pulse voltammetry; EIS, Electrochemical impedance spectroscopy; GCE, Glassy carbon electrode; GOx, Glucose oxidase; HRP, Horseradish peroxidase; ITO, Indium tin oxide; LSPR, Localized surface plasmon resonance; QD, Quantum dots; SPCE, Screen-printed carbon electrode; SPR, Surface plasmon resonance.

[a] Value was expressed in $\mu g\ mL^{-1}$/$ng\ mL^{-1}$/$pg\ mL^{-1}$ and converted to nM.

[b] The results were not possible to be converted to molar units thus being displayed in $pg\ mL^{-1}$.

3.2.1. *Aβ and related variants*

A lot of studies focus their efforts in Aβ detection (Table 1) as this peptide is considered to be the main pathological feature of AD. Aβ42 is the sequence more prone to aggregate thus being the peptide with more expression in the amyloid plaques making it a very interesting and important biomarker to study AD onset and progression. From Table 1, it is possible to conclude that a large number of the developed biosensors were able to successfully quantify Aβ42 below the cut-off value of 110–155 pM (500–700 pg mL^{-1}) in CSF [35,81], but colorimetric [82] and fluorescent [80] detection systems were not able to attain limits of detection (LODs) as low as the other systems. In addition, it is important to point out that five works were able to attain extremely low LODs achieving values lower than dozens of fM (Table 1) [71,77,79,83,91]. Three of these studies [71,77,91] determined trace level concentrations of Aβ42 through analysis of impedance variation.

Yoo et al. [71] developed a biosensor based on a microfluidic platform with interdigitated microelectrodes that comprised an ion concentration polarization preconcentration element that increased the local concentration of analytes and consequently improved the determination of Aβ42. The monoclonal antibodies were immobilized on the polyvinyl pyrrolidone-aldehyde and glutaraldehyde modified surface via interaction with aldehyde groups. Through changes in the impedance signal, this group was able to measure concentration levels as low as 2.2×10^{-3} – 221 pM achieving a LOD of 8.15 fM in buffer. Despite achieving very interesting detection levels for AD diagnosis, the performance of this biosensor in terms of stability and specificity was not evaluated. Wu et al. [77] attained a LOD of 2.2 fM for Aβ42 determination via EIS using a nanostructured label-free biosensing platform based on an AAO substrate modified with uniformly deposited AuNPs and 11-mercaptoundecanoic acid self-assembled monolayer (SAM) that was further functionalized with antibodies via EDC/NHS interaction [77]. The high surface-to-volume ratio of the AuNPs enabled the immobilization of more antibodies onto the electrode. For detection of Aβ42, this team [77] used a 30 μL sample volume with a detection period of 30 min attaining a linear detection range between 0.22 and 2200 pM in buffer. Despite achieving an extremely low LOD, the stability of the biosensor over time as well as its performance in real samples were not reported. Another very sensitive electrochemical biosensor for Aβ oligomers determination was designed by Qin et al. [91]. In this work, the developed biosensor was based on a AuE modified with an electrically conductive polypyrrole containing carboxyl groups for linking of the biorecognition agent, an amine modified PrP^C while also promoting the electron transfer for the electrochemical analysis. Applying the developed biosensor for Aβ oligomers detection, a 0.1 fM LOD was reached through EIS, while differentiating Aβ oligomers from monomers and fibrils, in addition to providing reliable performance in brain samples of AD infected mice [91]. Moreover, the developed electrochemical immunosensor presented no significant changes in signal after one month storage at 4 °C. In a different electrochemical approach, Zhao et al. [79] developed a dual quenching electrochemiluminescence (ECL) immunosensor which was based on a $Ru(bpy)_3^{2+}$ chromophore coupled with zinc oxalate metal-organic frameworks (MOFs) and a second MOFs with a nanocube structure composed of AuNPs-NiFe that acted as the dual quencher for sensitive detection of Aβ42. In this work, the $Ru(bpy)_3^{2+}$ cations were entrapped in a zinc oxalate MOFs with a 3D cage structure with the goal of increasing the energy transfer between $Ru(bpy)_3^{2+}$ units while shielding the electronic structure of the chromophore which led to high-energy Ru emission efficiency [79]. This way, for the immunosensor development $Ru(bpy)_3^{2+}$/zinc oxalate MOFs were conjugated with antibodies via EDC/NHS interaction being the bioconjugate further immobilized on the surface of a GCE. After the Aβ42 biorecognition process another bioconjugate composed of AuNPs-NiFe MOFs was added to the modified transducer to complete the sandwich immunoassay. The AuNPs-NiFe acted as the dual quencher as the UV–Vis absorption spectra of this composite overlapped with the ECL emission spectra of the Ru

Table 4
Configuration, analytical performance and application of the developed biosensors for multiplexed detection of AD biomarkers.

Biomarker	Transducer	Detection Method	Sample	**Detection Range (nM)**	**LOD (nM)**	References
Aβ40 Aβ42	AuE modified with MPA SAM and antibodies which were later conjugated with Aβ(1–16)-heme-AuNPs	Competitive assay - CV	Buffer and aCSF	0.02–150	0.01	[112]
Aβ42 t-Aβ	AuE modified with MPA SAM, antibodies and biotinylated Aβ/ streptavidin- conjugated ALP	Competitive amperometric detection using p-aminophenol redox cycling	Buffer and aCSF	Aβ42) 0.5–50 t-Aβ) 0.05–5	5×10^{-3}	[113]
Aβ40/Aβ42	GCE modified with MWCNTs, AuNPs and Gelsolin	Sandwich Immunoassay using AuNPs modified with gelsolin and HRP for DPV signal amplification	Buffer, CSF and brain tissue of rats	0.1–50	0.028	[114]
Aβ40 Aβ42	Triple barrel carbon fiber microelectrodes functionalized with antibodies through EDC/NHSS coupling	SWV – Oxidation of Aβ through a Tyrosine residue	Mice CSF	Aβ40) 20-50 Aβ42) 20-140	20	[115]
Aβ40 Aβ42	Microelectrode modified with conductive silk fibroin based immunoparticles through one-step electrophoresis/ electropolymerization	Linear Sweep Voltammetry	Buffer and Serum	Aβ40) 2.1×10^{-3} – 0.52[a] Aβ42) 4.9×10^{-3} – 0.25[a]	Aβ40) 1.53×10^{-3}[a] Aβ42) 8.8×10^{-4}[a]	[116]
Aβ40/Aβ42	Au films coated onto glass slides functionalized with mixed SAM composed of carboxyl- and hydroxyl-terminated PEG molecules, streptavidin and biotinylated antibodies	Sandwich Immunoassay through the conjugate preformed between biotinylated Aβ(1–16) antibody and streptavidin - SPR	Buffer and CSF	0.02–1	0.02	[117]
Aβ40/Aβ42	AgNPs modified with antibodies against Aβ40/Aβ42	Colorimetric detection through coupling of modified AgNPs with Cu^{2+}	Buffer and Human blood serum	0.25–150	0.086	[118]
Aβ40 Aβ42 Tau Protein	APTES-coated glass modified with immuno-PEG-AuNPs functionalized with antibodies through EDC/NHS	LSPR	Dulbecco's PBS mixed with human plasma samples	1×10^{-5} – 100	Aβ40) 3.49×10^{-5}; Aβ42) 2.6×10^{-5}; Tau protein) 2.36×10^{-5}	[119]
Aβ ApoE	SPCE modified with porous magnetic microspheres functionalized with antibodies through EDC/NHS, antigen and AuNPs functionalized with antibodies through adsorption due to the presence of cysteine	Sandwich immunoassay - Chronoamperometry	Buffer, CSF, serum and plasma samples of AD patients	Aβ) 4.4×10^{-3} – 2.8[a] ApoE) 2.9×10^{-3} – 0.37[a]	Aβ) 4.2×10^{-3}[a] ApoE) 2.4×10^{-3}[a]	[120]
1) H_2O_2; Aβ 2) Glutamate; Acetylcholine	Glass microscope slides coated with sol-gel derived optical array modified with: 1) Amplex red and FITC-dextran with HRP for H_2O_2 and Aβ detection 2) Glutamate dehydrogenase and acetylcholinesterase combined with carboxy SNARF-1-dextran for glutamate and acetylcholine detection	Fluorescent detection	3-bis [tris (hydroxymethyl) methylamino] propane buffer and Human serum	1) H_2O_2) 100–10^7; Aβ) 2.2–22200[a] 2) Glutamate) 5000–5×10^6; Acetylcholine) 5000–9×10^6	1) 1.57; 0.63 2) 530; 1020	[121]

aCSF, Artificial cerebrospinal fluid; AD, Alzheimer's disease; AgNPs, Silver nanoparticles; ALP, Alkaline phosphatase; APTES, 3-aminopropyltriethoxysilane; AuE, Gold electrode; AuNPs, Gold nanoparticles; CSF, Cerebrospinal fluid; CV, Cyclic voltammetry; DPV, Differential pulse voltammetry; EDC, 1-ethyl-3-(3-dimethylaminopropyl) carbodiimide; EIS, Electrochemical impedance spectroscopy; FITC, Fluorescein isothiocyanate; GCE, Glassy carbon electrode; HRP, Horseradish peroxidase; LSPR, Localized surface plasmon resonance; MPA, Mercaptopropionic acid; MWCNTs, Multi-walled carbon nanotubes; NHS, N-hydroxysuccinimide; NHSS, N-hydroxysulfosuccinimide; PBS, Phosphate buffered saline; PEG, Polyethylene glycol; SAM, Self-assembled monolayer; SPCE, Screen-printed carbon electrodes; SPR, Surface plasmon resonance; SWV, Square-wave voltammetry; t-Aβ, Total Aβ.

[a] Value was expressed in $\mu g\ mL^{-1}$/$ng\ mL^{-1}$/$pg\ mL^{-1}$ and converted to nM.

$(bpy)_3^{2+}$/zinc oxalate MOFs which would trigger the resonance energy transfer behavior achieving a dual quenching effect of the encapsulated $Ru(bpy)_3^{2+}$ and significantly increasing the sensitivity of the immunosensor [79]. With the developed strategy, Aβ42 was detected in the 0.022–1110 pM range while achieving a 3.0 fM LOD in buffer in addition to successfully analyzing the immunosensor in artificial CSF. Nonetheless, the stability of the immunosensor over time should be further tested. At last, Kang et al. [83] developed a vertically configured electrical detection system based on a different technique, namely STM, to evaluate a sandwich immunoassay for Aβ42 determination [83]. A biosurface was fabricated containing monoclonal antibody fragments, target protein and AuNPs-antibody conjugates for ultra-sensitive detection of Aβ42. The electrical tunneling current between the STM tip and the formed immunocomplexes exhibited a peak-like pulse, the frequency of which depended on the density of the bound complexes on the surface which enable the detection of levels as low as 2.2 fM in buffer. Nevertheless, this highly sensitive biosensor needs further optimizations related with stability and specificity in order to assess its viability for clinical application [83].

Biosensors based on optical determination, particularly LSPR [84] and SPR [85], have also been applied to detect and measure Aβ42 levels in biological fluids. Using LSPR, Kang et al. [84] performed Aβ42 quantification under physiological conditions. The developed system was a label-free biosensor based on AuNPs and ApoE4-mediated Aβ aggregation, where AuNPs acted as a catalytic activator and optical reporter while ApoE4 acted as a chaperon to monitor Aβ42 aggregation (Fig. 1), attaining a LOD of 1.5 pM [84]. Moreover, this work also demonstrated that ApoE4 induces Aβ42 aggregation more specifically and rapidly than that of Aβ40. In another work for Aβ42 quantification via SPR, Lee et al. [85] developed a biosensor based on a waveguide-coupled bimetallic chip (WcBiM) modified with antibodies via EDC/NHS covalent binding (Fig. 2). The line width of the reflectance for the WcBiM chip was narrower than the line width of the conventional Au chip resulting in a steeper gradient to maximize the resolution in the intensity detection mode. Application of this biosensor led to Aβ42 determination in the 22.2–443.1 pM range, although presenting limitations for detecting trace levels concentrations. In addition, both these studies did not evaluate the biosensors performance after exposure to real samples despite the first study conducting the entire work in mimicked CSF.

In recent studies, with the goal of overcoming some limitations related with the use of antibodies towards detection of biomarkers particularly in complex samples such as CSF and blood, biosensors were developed based on electrochemical determination towards Aβ detection without biological recognition elements. This way, Zhu et al. [132] developed an antibody-mimetic self-assembling peptoid nanosheet containing surface exposed Aβ42 recognizing loops which enabled a sensitive and label-free detection of AD in serum. In a different work, Qin et al. [133] prepared a ferrocene-encapsulated Zn zeolitic imidazole framework (ZIF-8) by self-assembly of Zn ions and 2-methylimidazole for detection of Aβ oligomers. Ferrocene, an optically and electrochemical active signal, was successfully encapsulated inside of

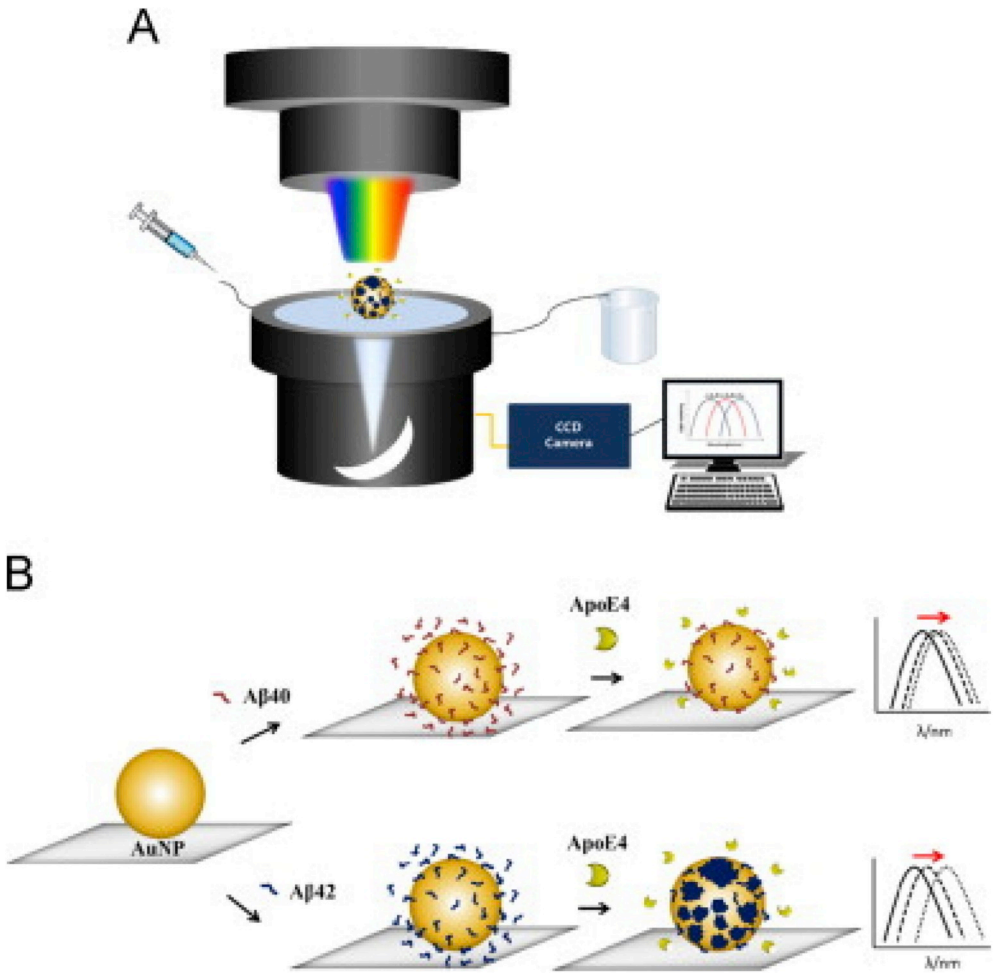

Fig. 1. (A) Schematic of the overall process describing the system setup by LSPR. (B) Experimental process for binding affinity [84]. Reprinted from Biosensors and Bioelectronics, 72, Min Kyung Kang, Jeewon Lee, Anh H. Nguyen, Sang Jun Sim, Label-free detection of ApoE4-mediated β-amyloid aggregation on single nanoparticle uncovering Alzheimer's disease, 197–204, Copyright (2015), with permission from Elsevier.

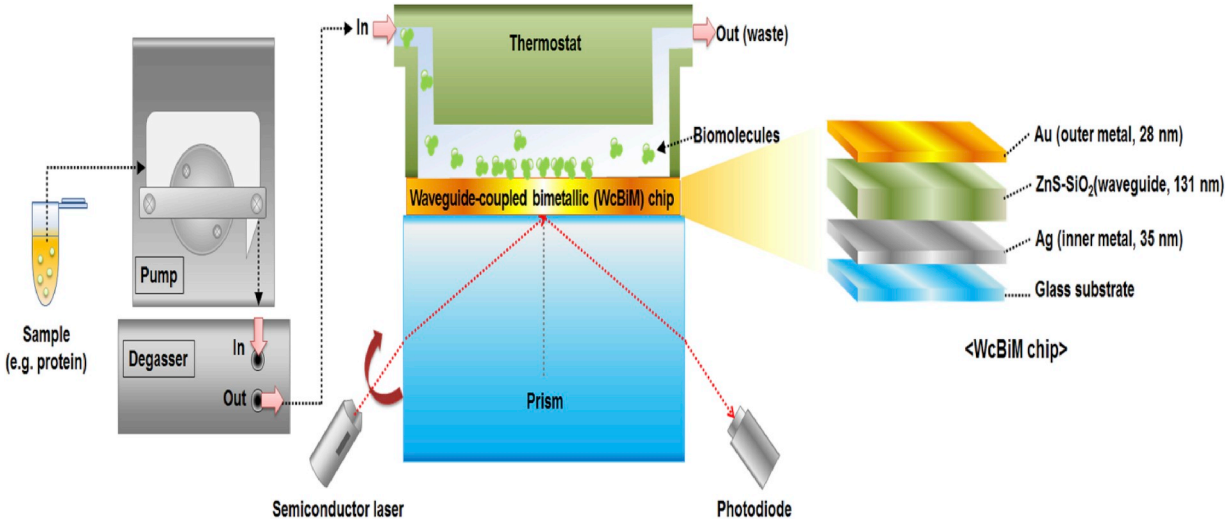

Fig. 2. Schematic diagram of the SPR sensor system and the Waveguide-coupled bimetallic chip configuration [85]. Reprinted from Y.K. Lee, K.-S. Lee, W.M. Kim, Y.-S. Sohn, (2014) Detection of Amyloid-β42 Using a Waveguide-Coupled Bimetallic Surface Plasmon Resonance Sensor Chip in the Intensity Measurement Mode. PLoS ONE 9(6): e98992. Copyright (2014), with permission from Plos.

the ZIF-8 and released by the competitive coordination between Zn ions and Aβ oligomers [133].

3.2.2. Tau protein

Electrochemical biosensors have also been the most applied for determination of tau protein [94–99] (Table 2). On the other hand, five works displayed in Table 2 were based on different techniques namely, LSPR [100], SPR [101–103] and QCM [104]. Clinical application of tau protein can be very challenging as its cut-off value in CSF is 4.3 pM [96,100,134]; of the reported eleven studies, five biosensors (two electrochemical [96,98] and three optical [100–102]) fulfilled this requirement.

Applying EIS for determination of full-length 2N4R tau protein, Wang et al. [96] were able to measure values in the fM range exhibiting better performance when compared to enzyme-linked immunosorbent assays (ELISA) by achieving a 30 fM LOD with a detection period of 25 min. The developed biosensor was based on four gold microband electrodes modified with a layer of 3,3′-dithiobis(sulfosuccinimidyl propionate) and protein G for immobilization of antibodies with proper orientation [96]. In another electrochemical approach for tau protein-381 detection in human serum, Shui et al. [98] developed a sandwich assay based on the interaction between tau protein and respective antibodies and aptamers, performing detection in the 0.5–100 pM range and attaining a LOD of 0.42 pM with a 45 min incubation period at room temperature. Antibodies were immobilized on a mercaptopropionic acid SAM modified gold electrode while the aptamers where conjugated with gold nanoparticles to complete the sandwich assay. AuNPs played a dual role of enhancing the electrochemical behavior of the biosensor, for a more sensitive determination of tau protein, while offering a suitable matrix for the immobilization of aptamers. Both these biosensors were successfully tested in human serum spiked with tau protein but to confirm their applicability to clinical analysis, their performance over time should be evaluated.

Three biosensors based on LSPR and SPR exhibited detection limits lower than tau protein physiological level [100–102]. A method centered on the conjugation of affinity-based biosensing and LSPR multi-spot nanoparticle chip was employed for the detection of tau protein at room temperature [100]. In this work, Vestergaard et al. [100] modified a glass chip with a chromium and gold layer that was further functionalized with a 4,4-dithiodibutyric acid SAM, amino-surface modified silica nanoparticles, another gold layer to cap the nanoparticles and finally protein G to promote the antibodies immobilization with proper orientation. With this method, the authors were able to attain a 0.17 pM LOD in buffer. Despite achieving a low detection limit, this work involved longer incubation periods and the biosensor performance was not evaluated in real samples. In a more recent study, Thi Vu Nu et al. [101] presented an immunoassay for the detection of both total tau and phosphorylated tau protein based on a gold coated fiber core functionalized with an 11-mercaptoundecanoic acid SAM, where the carboxylic groups were activated via EDC/NHS interaction to promote immobilization of the respective antibodies. Using SPR, detection limits of 0.53 fM for total tau and 1.3 pM for phosphorylated tau were achieved in addition to determining its levels in human blood. Moreover, this study concluded that the concentration of total tau protein in AD groups was six times higher than that of controls while phosphorylated tau was three times higher [101]. This difference of concentration between the two types of tau protein was attributed to the fact that unphosphorylated tau is more likely to be produced in blood than the phosphorylated protein [101]. In another work based on a multichannel SPR platform, Kim et al. [102] introduced a DNA aptamer/antibody pairing sandwich assay specific for tau-381 and applied it for detection of human Tau in undiluted human plasma quantifying levels within the range 2–80 pM and attaining a detection limit of femtomolar concentration. The DNA aptamer was immobilized on a gold chip modified with a mixed monolayer of 11-mercaptoundecanoic acid and 11-mercaptoundecanol through EDC/NHSS covalent linking. After tau protein specific adsorption, antibodies were flowed through the modified gold chip surface leading to the formation of a sandwich immunocomplex which increased the SPR detection signal. Both these studies [101,102] did not address the period of stability of the developed biosensors, which is a crucial parameter to ensure that a biosensor can perform with *ca.* the same efficiency over time.

3.2.3. ApoE

ApoE is another target biomarker for which mostly electrochemical biosensors have been developed; only one work was based on a different technique (colorimetric detection) (Table 3). Three of the electrochemical biosensors determined ApoE through evaluation of DNA hybridization at a specific point mutation in the ApoE gene [106,109,110] and two of these works used two techniques to study this event. Mars et al. [109] used DPV and fluorescent detection while Cheng et al. [110] performed its evaluation through EIS and LSPR. In both cases, the biosensors performance was better when evaluated

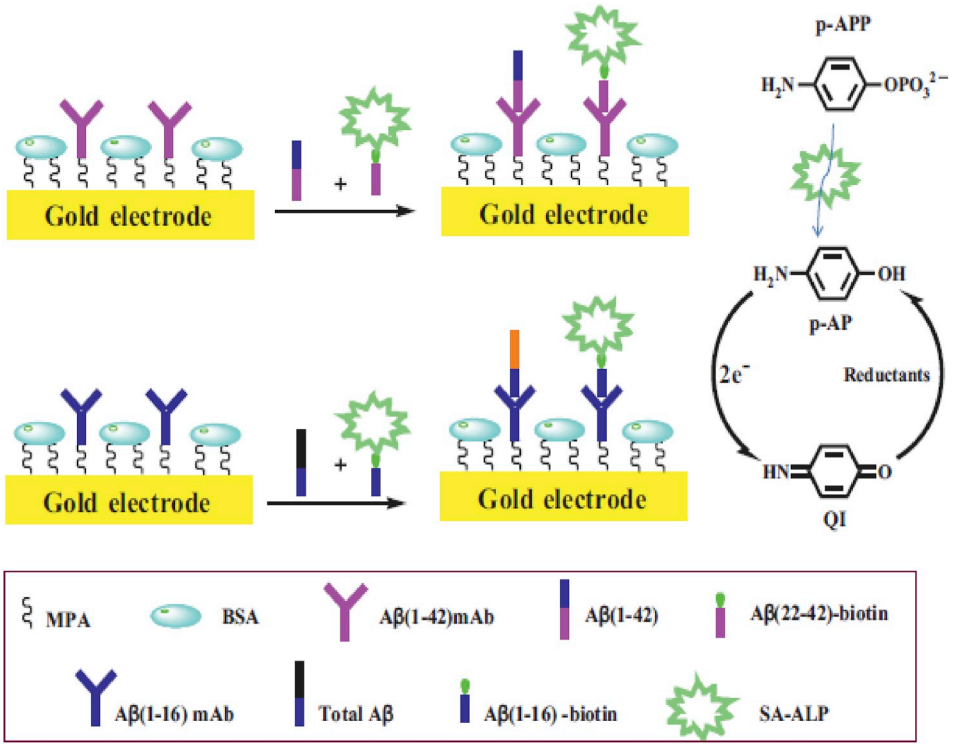

Fig. 3. Schematic representation for the detection of Aβ(1–42) and total Aβ using p-amino phenol redox cycling by chemical reductants [113]. Reprinted from Biosensors and Bioelectronics, 51, M L. Liu, Q. He, F. Zhao, N. Xia, H. Liu, S. Li, R. Liu, H. Zhang, Competitive electrochemical immunoassay for detection of β-amyloid (1–42) and total β-amyloid peptides using p-aminophenol redox cycling, 208–212, Copyright (2014), with permission from Elsevier.

through electrochemical techniques demonstrating once again their high sensitivity. Beyond DPV and EIS, other electrochemical techniques have been efficient for determination of biomarkers such as square wave anodic stripping voltammetry, which was applied by Medina-Sánchez et al. [107] for ApoE detection. The developed biosensor consisted on a microfluidic system with integrated SPEs where the immunocomplex was performed using magnetic beads for a pre-concentration step and QDs as labeling carriers [107]. QDs are semiconductor nanoparticles which have been gaining increasing relevance in the biosensing field, mainly applied with a labelling function, due to their optical properties and stability in addition to presenting interesting electrochemical properties [57,66,107]. Therefore, magnetic beads were coupled with antibodies and immobilized on the electrode surface by using a neodymium magnet placed underneath the substrate. Then, biotinylated ApoE was flushed through the magnetic beads followed by QDs conjugated with streptavidin to complete the magneto immunocomplex. Applying an incubation period of 10 min, this system attained a LOD of 0.37 nM with a linear range from 0.29 to 5.9 nM through measurement of the QDs signal, while also demonstrating high accuracy in diluted human plasma [107]. Stability assays should be further carried out as this is a crucial parameter.

The only work that did not perform ApoE determination through electrochemical techniques was reported by Ren et al. [111] that presented a colorimetric immunosensor with one of the lowest LODs (12 fM) being its performance evaluated in buffer and human serum (Table 3). The biosensor was based on a sandwich assay and was developed in a layer-by-layer approach [111]. Firstly, the ITO surface was modified with a 3-aminopropyltrimethoxysilane and glutaraldehyde conjugate, which exhibited a brick-red color that faded when oxidized by H_2O_2. Then, a second conjugate composed of an ionic liquid ($BMIMBF_4$) and chitosan was incubated in the surface to stabilize the first layer. Lastly, to promote the immobilization of the antibodies through amine binding, AuNPs were added to the modified ITO surface. To complete the sandwich assay, a nanocomposite of AuNPs/TiO_2 modified with antibodies and glucose oxidase was used to perform the biomarker quantification [111]. As a final step, glucose was dropped on the immunosensor surface being catalyzed by the glucose oxidase to produce H_2O_2 promoting the respective color fading that was further evaluated through an image processing software by performing quantification of its mean gray value. Despite displaying good analytical behavior, further assays related to reproducibility and stability parameters need to be carried out.

3.2.4. *Multiplexed detection*

As already referred, AD is affected by multifactorial pathways that lead to changes at biomolecular levels as the disease progresses [2,8,9]. Thus, an accurate diagnosis of AD should arise from the evaluation of a combination of core biomarkers such as the quantification of Aβ42 and Aβ40 and respective assessment of their concentration ratio [8], in conjunction with determination of tau protein or ApoE or even both [8]. In this context, seven works (Table 4) reported the development of biosensors for the determination of Aβ40 and Aβ42; as for the individual biomarker analysis, electrochemical detection [112–116] was preferred over other strategies [117,118]. All of the seven works described in Table 4 for Aβ40/Aβ42, with exception for one [115], were able to attain LODs in the pM range; in addition, five works also evaluated the performance of the developed biosensors in real samples [114–118]. From the seven biosensors, three performed determination of Aβ40/Aβ42 through a competitive assay [112,113,116], two via a sandwich assay [114,117] and two accomplished direct determination of the analytes [115,118].

A competitive immunoassay using *p*-aminophenol (*p*-AP) redox cycling was described by Liu et al. [113] for detection of both Aβ42 and total Aβ. Specifically, the interaction between biotinylated Aβ peptides already captured by the antibodies immobilized on the mercaptopropionic acid modified gold electrodes and the conjugate streptavidin-modified alkaline phosphatase (SA-ALP) induced the production of electrochemically active *p*-AP from the *p*-aminophenyl phosphate (p-APP) substrate (Fig. 3) [113]. The proposed electrochemical immunosensor was able to detect levels of 5 pM for both Aβ42 and total Aβ. Moreover, the authors [113] concluded that artificial cerebrospinal fluid (aCSF) had no interference in the analysis. Yu et al. [114] by means of a sandwich-type biosensor array was able to simultaneously quantify Aβ40/Aβ42, developing a transducer platform based on a GCE

modified with MWCNTs, AuNPs and using gelsolin as the biorecognition element, which is a secretory protein with high specificity towards Aβ monomers. MWCNTs and AuNPs due to their excellent conductivity and electrochemical properties enhanced the electrochemical behavior of the biosensor by increasing the charging currents in addition to providing an appropriate environment for the immobilization of gelsolin. AuNPs were also used for signal amplification by coupling them with gelsolin and horse-radish peroxidase (HPR) to complete the sandwich immunoassay. Electrochemical signal was amplified via enormous loading of HRP on the AuNPs which could catalyze the substrate 3,3′,5,5′-tetramethylbenzidine in the presence of H_2O_2 to produce measurable redox currents [114]. Using the proposed biosensor, the research team [114] was able to attain a 28 pM LOD in spiked buffer in addition to successfully determine Aβ40/Aβ42 in CSF and in three different brain tissues of rats, observing a clear decline in the concentrations of soluble Aβ40/Aβ42 of AD rats as a result of Aβ aggregation. Despite exhibiting sensitive and specific determination of Aβ40/Aβ42, the proposed biosensor requires long incubation periods while displaying only two weeks stability when stored at 4 °C. In a different approach, Liu et al. [116] developed a hierarchical immunoelectrochemical interface based on a microelectrode nanostructured with conductive silk fibroin (SF)-based immunoparticles via an one-step electrophoresis/electropolymerization. Antibody conjugation was promoted through the interactions with the hydrophilic N-terminal sites on the surface. This nanostructured conductive interface favored penetration of water-soluble biomolecules and catalyzed a redox reaction of Met(35) providing detection limits of 0.88 pM and 1.53 pM for Aβ42 and Aβ40, respectively. Moreover, the developed biosensor was successfully tested in real serum samples while only displaying two weeks stability when stored at 4 °C [116].

Low levels of Aβ40/Aβ42 were also detected by Xia et al. [117] via SPR. This work had the advantage of simultaneously, but separately, quantifying both peptides from CSF of AD patients by pre-immobilizing the respective antibodies onto two separate fluidic channels minimizing, this way, the non-specific determination (Fig. 4). Signal amplification was achieved by the formation of a conjugate between streptavidin and an antibody selective to the common N-terminus of Aβ peptides that were previously captured, leading to the measurement of concentrations as low as 20 pM. Furthermore, this study [117] revealed that the ratio between the concentrations of Aβ40 and Aβ42 in CSF samples from AD patients is almost twice as high as that from healthy persons. Comparing to more traditional methods such as ELISA, this method offered significant advantages by presenting faster analysis time, obviation of an enzyme-linked antibody for signal detection and regeneration of the biosensor surface for replicate measurements [117].

Despite exhibiting excellent performance through detection of low levels of Aβ, some of the works displayed [112–114] in Table 4 present the common disadvantage of lack of specificity of the biological recognition elements. Half of the designed biosensors for both Aβ40 and Aβ42 detection used antibodies capable of recognizing a broad range of amyloid beta peptides. Thus, the development of biorecognition elements capable of distinguishing different variants of a protein is a topic that requires more focus as it will contribute to better and more accurate diagnostic procedures.

For quantification of the AD core biomarkers, Kim et al. [119] using LSPR presented a highly selective shape-code biosensor based on a single platform modified with AuNPs of different shapes. These AuNPs were previously modified with polyethylene glycol (PEG) that through EDC/NHS interaction promoted stable antibody immobilization. AuNPs of different shapes and sizes, such as spheres (diameter of 50 nm), short rods (aspect ratio of 1.6) and long rods (aspect ratio of 3.6), exhibit different optical behaviors which could be identified and differentiated through LSPR as if a bar-code was being scanned. Applying a 1 h incubation period and under physiological conditions, this research team [119] reported a detection limit of 34.9 fM for Aβ40, 26 fM for Aβ42 and 23.6 fM for tau protein. A different conjugation of AD biomarkers was determined by de la Escosura-Muñiz et al. [120] that developed a biosensor based on a magnetosandwich-immunoassay for Aβ and ApoE determination in CSF, plasma and serum. In this work, porous magnetic microspheres were used for the antibody immobilization, which due to their inherent characteristics, allowed for a more efficient capture of the analyte while also providing a high active area for enhanced

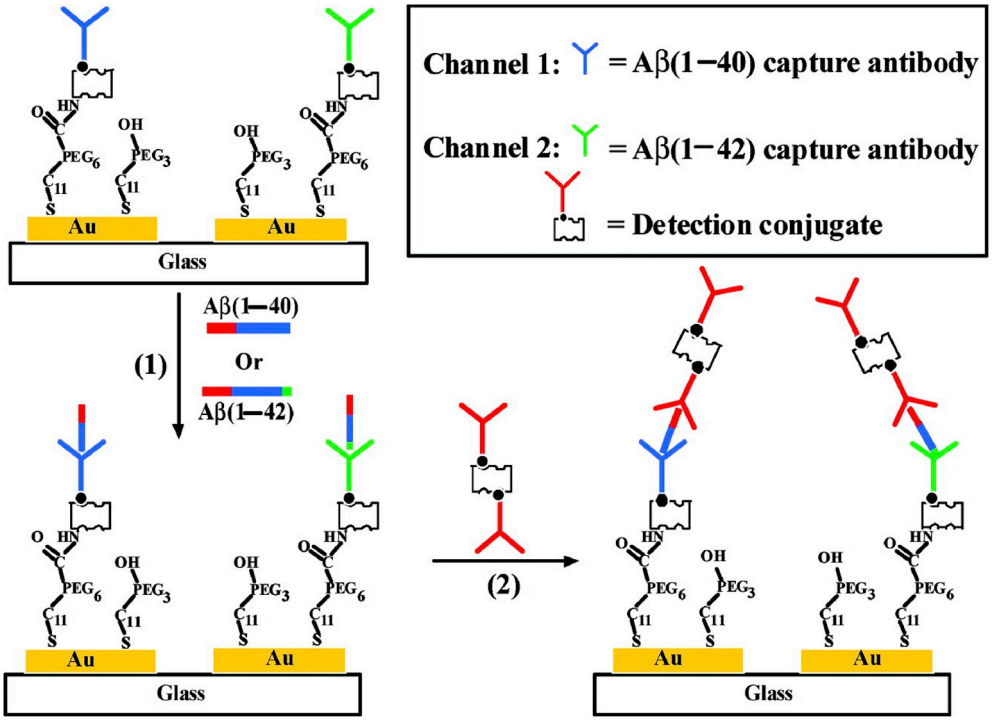

Fig. 4. Schematic diagram showing the simultaneous SPR detection of Aβ40 and Aβ42 [117]. Reprinted with permission from N. Xia, L. Liu, M.G. Harrington, J. Wang, F. Zhou, Analytical Chemistry, 82 (2010) 10151–10157. Copyright (2010) American Chemical Society.

catalytic activity of the conjugate detection-antibody/AuNPs [120]. AD biomarkers were added to the microspheres modified with the capture antibodies, being the detection performed through the conjugate detection antibody/AuNPs. The magnetic conjugate suspension was placed on the surface of a SPCE and analyzed through chronoamperometry presenting a LOD of 4.2 pM for Aβ and 2.4 pM for ApoE. The detection process involved two immunoreaction stages that were carried out for 20 min at 25 °C each.

The possibility of performing detection of multiple biomarkers in a single platform brings the proposed biosensors closer to real clinical diagnosis being the focus of recent studies [135]. Moreover, despite centering primarily on the main biomarkers of AD such as Aβ42, Aβ40 and t-tau and p-tau, other studies have also performed detection of multiple analytes that extend beyond this main core of biomarkers such as Aβ and phosphorylated Aβ [136], tau protein and alpha-1-antitrypsin [137,138], Aβ, glutamate and acetylcholine [121].

4. Conclusion

The ageing of the World's population is poised to become one of the biggest social challenges of the 21st century. Specifically, this event may promote the increase in AD prevalence, which will impose a high financial burden on societies, as this condition extends itself through years with high costs associated to treatment and caring for elderly. Currently, there are no simple and reliable diagnostic tests for AD. It remains essentially a clinical diagnosis, subject to variations in patient presentation and physician assessment, which can lead to errors as several dementias and movement disorders often feature clinical similarities making their differential diagnosis (especially in the early stages) extremely challenging. Therefore, with the emergence of specific therapeutic interventions, there is an ever-increasing demand for the development of simple and accurate diagnostic tools, such as biosensors, to assist the medical community to establish the best course of action for each specific case.

Reviewing the works developed throughout the last decade concerning the detection of AD biomarkers in human fluids, it was possible to identify some topics that should be further developed. Firstly, most of the reported biosensors are only able to determine one single biomarker. As AD is considered to be a multifactorial disorder resulting from a combination of multiple pathological pathways, there is an urgent need to adapt current biosensing technology into single platforms capable of performing multiplexed determination. This feature will simplify the detection process while speeding it, lowering its costs and improving the quality of the diagnostic procedures. In addition, the simultaneous detection of these biomarkers will ensure that a specific condition is accurately detected and differentiated from the others thus, minimizing the risk of misdiagnosis. Another common feature in the reported biosensors is the lack of specificity of the biological recognition elements. Part of the designed biosensors for both Aβ40 and Aβ42 detection used antibodies capable of recognizing a broad range of amyloid beta peptides. Therefore, the development of biorecognition elements capable of distinguish different variants of a protein is a topic that requires more attention as it will contribute to better and more accurate diagnostic procedures. Another issue that needs to be overcome, as it can compromise the robustness and analytical performance of biosensors, is the biofouling of their surface that frequently occurs when complex matrices are used. Biofouling describes the chronic formation of a biofilm on the biosensor surface through protein adsorption, causing the impairment of the device function particularly in its capability of conducting long-term measurements.

An additional element associated with the development of biosensors resonates with the relevance achieved by nanomaterials which, due to their inherent characteristics, have become an intricate part of each biosensor system. Nanostructured materials have highly specific physical and chemical properties due to quantum-size effects and large surface areas, which provide them unique and different properties compared to bulk materials. A diversity of nanomaterials can be produced by several synthetic methodologies with well-controlled physicochemical properties as surface charge, shape and size. The application of these nanomaterials in bioanalytical devices will continue to improve their sensitivity and detection limits down to pico- and even femto-molar levels.

The biosensing technology is diligently developing towards the production of point-of-care technology capable of performing accurate and sensitive determination of key AD biomarkers in biological fluids. Future studies should be focused on the development of technology capable of bridging the gap between studies and clinical application through the development of single platforms capable of performing multiplexed analysis with excellent sensitivity, specificity and stability, while achieving all these characteristics through the use of lower sample volumes and with shorter detection periods, which will hopefully culminate in the commercialization and clinical application of these biosensors.

Conflict of interest

The authors declare no conflict of interest.

Acknowledgments

This work was financially supported by: project UID/EQU/00511/2019 - Laboratory for Process Engineering, Environment, Biotechnology and Energy – LEPABE and project UID/QUI/50006/2019 – REQUIMTE, both funded by national funds through FCT/MCTES (PIDDAC); Project POCI-01-0145-FEDER-006939, funded by FEDER funds through COMPETE2020 - *Programa Operacional Competitividade e Internacionalização* (POCI) and by national funds (PIDDAC) through FCT/MCTES; Project "LEPABE-2-ECO-INNOVATION" – NORTE-01-0145-FEDER-000005, funded by Norte Portugal Regional Operational Programme (NORTE 2020), under PORTUGAL 2020 Partnership Agreement, through the European Regional Development Fund (ERDF). PhD grant financially supported by Fundação para a Ciência e Tecnologia (SFRH/BD/131755/2017).

References

[1] M. Goedert, Science (New York, N.Y.) (2015) 349.
[2] P. Scheltens, K. Blennow, M.M. Breteler, B. de Strooper, G.B. Frisoni, S. Salloway, W.M. Van der Flier, Lancet (London, England) 388 (2016) 505–517.
[3] L.V. Kalia, A.E. Lang, The Lancet 386 (2015) 896–912.
[4] H.V.S. Ganesh, A.M. Chow, K. Kerman, Trac. Trends Anal. Chem. 79 (2016) 363–370.
[5] Alzheimer's Dementia 14 (2018) 367–429.
[6] A. Kumar, A. Singh, Ekavali, Pharmacological Reports 67 (2015) 195–203.
[7] J.L. Cummings, Alzheimer's & dementia: J. Alzheimer's Assoc. 7 (2011) e13–44.
[8] J.L. Molinuevo, S. Ayton, R. Batrla, M.M. Bednar, T. Bittner, J. Cummings, A.M. Fagan, H. Hampel, M.M. Mielke, A. Mikulskis, S. O'Bryant, P. Scheltens, J. Sevigny, L.M. Shaw, H.D. Soares, G. Tong, J.Q. Trojanowski, H. Zetterberg, K. Blennow, Acta Neuropathol. 136 (2018) 821–853.
[9] C.L. Masters, R. Bateman, K. Blennow, C.C. Rowe, R.A. Sperling, J.L. Cummings, Nature reviews. Disease primers 1 (2015) 15056.
[10] C. Ballard, S. Gauthier, A. Corbett, C. Brayne, D. Aarsland, E. Jones, Lancet (London, England) 377 (2011) 1019–1031.
[11] K. Blennow, M.J. de Leon, H. Zetterberg, Lancet (London, England) 368 (2006) 387–403.
[12] C.A. Lane, J. Hardy, J.M. Schott, Eur. J. Neurol. 25 (2018) 59–70.
[13] J. Wang, B.J. Gu, C.L. Masters, Y.-J. Wang, Nat. Rev. Neurol. 13 (2017) 612.
[14] H. Hampel, Y. Shen, D.M. Walsh, P. Aisen, L.M. Shaw, H. Zetterberg, J.Q. Trojanowski, K. Blennow, Exp. Neurol. 223 (2010) 334–346.
[15] W.V. Graham, A. Bonito-Oliva, T.P. Sakmar, Annu. Rev. Med. 68 (2017) 413–430.
[16] H. Zetterberg, K. Blennow, E. Hanse, Exp. Gerontol. 45 (2010) 23–29.
[17] V. Calsolaro, P. Edison, Alzheimer's & dementia: J. Alzheimer's Assoc. 12 (2016) 719–732.
[18] D.J. Selkoe, J. Hardy, EMBO Mol. Med. 8 (2016) 595–608.
[19] K.L. Viola, W.L. Klein, Acta Neuropathol. 129 (2015) 183–206.
[20] C.C. Rowe, P. Bourgeat, K.A. Ellis, B. Brown, Y.Y. Lim, R. Mulligan, G. Jones, P. Maruff, M. Woodward, R. Price, P. Robins, H. Tochon-Danguy, G. O'Keefe, K.E. Pike, P. Yates, C. Szoeke, O. Salvado, S.L. Macaulay, T. O'Meara, R. Head, L. Cobiac, G. Savage, R. Martins, C.L. Masters, D. Ames, V.L. Villemagne, Ann.

Neurol. 74 (2013) 905–913.
[21] T.L. Spires-Jones, J. Attems, D.R. Thal, Acta Neuropathol. 134 (2017) 187–205.
[22] H.G. Lee, G. Perry, P.I. Moreira, M.R. Garrett, Q. Liu, X. Zhu, A. Takeda, A. Nunomura, M.A. Smith, Trends Mol. Med. 11 (2005) 164–169.
[23] T. Arendt, J.T. Stieler, M. Holzer, Brain Res. Bull. 126 (2016) 238–292.
[24] R. Craig-Schapiro, A.M. Fagan, D.M. Holtzman, Neurobiol. Dis. 35 (2009) 128–140.
[25] W. Mair, J. Muntel, K. Tepper, S. Tang, J. Biernat, W.W. Seeley, K.S. Kosik, E. Mandelkow, H. Steen, J.A. Steen, Anal. Chem. 88 (2016) 3704–3714.
[26] G. Bu, Nature reviews, Neuroscience 10 (2009) 333–344.
[27] J.T. Yu, L. Tan, J. Hardy, Annu. Rev. Neurosci. 37 (2014) 79–100.
[28] P.B. Verghese, J.M. Castellano, D.M. Holtzman, The lancet, Neurology 10 (2011) 241–252.
[29] J. Kim, J.M. Basak, D.M. Holtzman, Neuron 63 (2009) 287–303.
[30] O. Hansson, J. Seibyl, E. Stomrud, H. Zetterberg, J.Q. Trojanowski, T. Bittner, V. Lifke, V. Corradini, U. Eichenlaub, R. Batrla, K. Buck, K. Zink, C. Rabe, K. Blennow, L.M. Shaw, Alzheimer's & dementia: J. Alzheimer's Assoc. 14 (2018) 1470–1481.
[31] C.R. Jack Jr., D.A. Bennett, K. Blennow, M.C. Carrillo, B. Dunn, S.B. Haeberlein, D.M. Holtzman, W. Jagust, F. Jessen, J. Karlawish, E. Liu, J.L. Molinuevo, T. Montine, C. Phelps, K.P. Rankin, C.C. Rowe, P. Scheltens, E. Siemers, H.M. Snyder, R. Sperling, Alzheimer's & dementia: J. Alzheimer's Assoc. 14 (2018) 535–562.
[32] B. Dubois, H.H. Feldman, C. Jacova, H. Hampel, J.L. Molinuevo, K. Blennow, S.T. DeKosky, S. Gauthier, D. Selkoe, R. Bateman, S. Cappa, S. Crutch, S. Engelborghs, G.B. Frisoni, N.C. Fox, D. Galasko, M.-O. Habert, G.A. Jicha, A. Nordberg, F. Pasquier, G. Rabinovici, P. Robert, C. Rowe, S. Salloway, M. Sarazin, S. Epelbaum, L.C. de Souza, B. Vellas, P.J. Visser, L. Schneider, Y. Stern, P. Scheltens, J.L. Cummings, Lancet Neurol. 13 (2014) 614–629.
[33] B. Olsson, R. Lautner, U. Andreasson, A. Ohrfelt, E. Portelius, M. Bjerke, M. Holtta, C. Rosen, C. Olsson, G. Strobel, E. Wu, K. Dakin, M. Petzold, K. Blennow, H. Zetterberg, The lancet, Neurology 15 (2016) 673–684.
[34] K. Blennow, H. Zetterberg, J. Intern. Med. 284 (2018) 643–663.
[35] O. Hansson, S. Lehmann, M. Otto, H. Zetterberg, P. Lewczuk, Alzheimer's Res. Ther. 11 (2019) 34.
[36] D.R. Thévenot, K. Toth, R.A. Durst, G.S. Wilson, Biosens. Bioelectron. 16 (2001) 121–131.
[37] M. Farré, L. Kantiani, D. Barceló, Chapter 7 - microfluidic devices: biosensors, in: Y. Picó (Ed.), Chemical Analysis of Food: Techniques and Applications, Academic Press, Boston, 2012, pp. 177–217.
[38] J. Kirsch, C. Siltanen, Q. Zhou, A. Revzin, A. Simonian, Chem. Soc. Rev. 42 (2013) 8733–8768.
[39] S.N. Sawant, 13 - development of biosensors from biopolymer composites, in: K.K. Sadasivuni, D. Ponnamma, J. Kim, J.J. Cabibihan, M.A. AlMaadeed (Eds.), Biopolymer Composites in Electronics, Elsevier, 2017, pp. 353–383.
[40] A.A. Zuber, E. Klantsataya, A. Bachhuka, 3.06 - biosensing, in: D.L. Andrews, R.H. Lipson, T. Nann (Eds.), Comprehensive Nanoscience and Nanotechnology, second ed., Academic Press, Oxford, 2019, pp. 105–126.
[41] S.K. Shukla, P.P. Govender, A. Tiwari, Chapter six - polymeric micellar structures for biosensor technology, in: A. Iglič, C.V. Kulkarni, M. Rappolt (Eds.), Advances in Biomembranes and Lipid Self-Assembly, Academic Press, 2016, pp. 143–161.
[42] M. Chakraborty, M. Saleem J Hashmi, An Overview of Biosensors and Devices, (2017).
[43] N.J. Ronkainen, H.B. Halsall, W.R. Heineman, Chem. Soc. Rev. 39 (2010) 1747–1763.
[44] F.J. Gruhl, B.E. Rapp, K. Lange, Adv. Biochem. Eng./Biotechnol 133 (2013) 115–148.
[45] A. Kawamura, T. Miyata, 4.2 - biosensors, in: M. Ebara (Ed.), Biomaterials Nanoarchitectonics, William Andrew Publishing, 2016, pp. 157–176.
[46] F.S. Felix, L. Angnes, Biosens. Bioelectron. 102 (2018) 470–478.
[47] G. Maduraiveeran, M. Sasidharan, V. Ganesan, Biosens. Bioelectron. 103 (2018) 113–129.
[48] D. Grieshaber, R. MacKenzie, J. Vörös, E. Reimhult, Sensors 8 (2008) 1400–1458.
[49] D.W. Kimmel, G. LeBlanc, M.E. Meschievitz, D.E. Cliffel, Anal. Chem. 84 (2012) 685–707.
[50] N. Jadon, R. Jain, S. Sharma, K. Singh, Talanta 161 (2016) 894–916.
[51] L. Syedmoradi, M. Daneshpour, M. Alvandipour, F.A. Gomez, H. Hajghassem, K. Omidfar, Biosens. Bioelectron. 87 (2017) 373–387.
[52] Z. Taleat, A. Khoshroo, M. Mazloum-Ardakani, Microchim Acta 181 (2014) 865–891.
[53] F. Arduini, L. Micheli, D. Moscone, G. Palleschi, S. Piermarini, F. Ricci, G. Volpe, Trac. Trends Anal. Chem. 79 (2016) 114–126.
[54] H.M. Mohamed, Trac. Trends Anal. Chem. 82 (2016) 1–11.
[55] H. Ju, X. Zhang, J. Wang, NanoBiosensing: Principles, Development and Application, Springer, New York, 2011.
[56] A. Walcarius, S.D. Minteer, J. Wang, Y. Lin, A. Merkoci, J. Mater. Chem. B 1 (2013) 4878–4908.
[57] Y. Chen, S. Zhou, L. Li, J.-j. Zhu, Nano Today 12 (2017) 98–115.
[58] C. Zhu, G. Yang, H. Li, D. Du, Y. Lin, Anal. Chem. 87 (2015) 230–249.
[59] J. Conde, J.T. Dias, V. Grazú, M. Moros, P.V. Baptista, J.M. de la Fuente, Frontiers in chemistry 2 (2014) 48-48.
[60] J.C. Claussen, J. Shi, C.S. Rout, M.S. Artiles, M.M. Roushar, M.C. Stensberg, D.M. Porterfield, T.S. Fisher, 3 - nano-sized biosensors for medical applications, in: S. Higson (Ed.), Biosensors for Medical Applications, Woodhead Publishing, 2012, pp. 65–102.
[61] A. Chen, S. Chatterjee, Chem. Soc. Rev. 42 (2013) 5425–5438.
[62] R.S. Luz, R. Iost, F. Crespilho, Nanomaterials for biosensors and implantable biodevices, in: F.N. Crespilho (Ed.), Nanobioelectrochemistry, Springer Berlin Heidelberg, 2013, pp. 27–48.
[63] F. Ricci, G. Adornetto, G. Palleschi, Electrochim. Acta 84 (2012) 74–83.
[64] Y. Wan, Y. Su, X. Zhu, G. Liu, C. Fan, Biosens. Bioelectron. 47 (2013) 1–11.
[65] W. Putzbach, N.J. Ronkainen, Sensors 13 (2013) 4811–4840.
[66] M. Holzinger, A. Le Goff, S. Cosnier, Frontiers in chemistry 2 (2014) 63-63.
[67] E. Steen Redeker, D.T. Ta, D. Cortens, B. Billen, W. Guedens, P. Adriaensens, Bioconjug. Chem. 24 (2013) 1761–1777.
[68] S.C.B. Gopinath, T.-H. Tang, M. Citartan, Y. Chen, T. Lakshmipriya, Biosens. Bioelectron. 57 (2014) 292–302.
[69] N. Stephanopoulos, M.B. Francis, Nat. Chem. Biol. 7 (2011) 876–884.
[70] J. Oh, G. Yoo, Y.W. Chang, H.J. Kim, J. Jose, E. Kim, J.C. Pyun, K.H. Yoo, Biosens. Bioelectron. 50 (2013) 345–350.
[71] Y.K. Yoo, D.S. Yoon, G. Kim, J. Kim, S.I. Han, J. Lee, M.-S. Chae, S.-M. Lee, K.H. Lee, K.S. Hwang, J.H. Lee, Sci. Rep. 7 (2017) 14303.
[72] Y.K. Yoo, J. Kim, G. Kim, Y.S. Kim, H.Y. Kim, S. Lee, W.W. Cho, S. Kim, S.M. Lee, B.C. Lee, J.H. Lee, K.S. Hwang, Sci. Rep. 7 (2017) 8882.
[73] Y. Yu, P. Wang, X. Zhu, Q. Peng, Y. Zhou, T. Yin, Y. Liang, X. Yin, Analyst 143 (2018) 323–331.
[74] F.S. Diba, S. Kim, H.J. Lee, Catal. Today 295 (2017) 41–47.
[75] E.C. Rama, M.B. González-García, A. Costa-García, Sens. Actuators B Chem. 201 (2014) 567–571.
[76] T.T.N. Lien, Y. Takamura, E. Tamiya, M.d.C. Vestergaard, Anal. Chim. Acta 892 (2015) 69–76.
[77] C.-C. Wu, B.-C. Ku, C.-H. Ko, C.-C. Chiu, G.-J. Wang, Y.-H. Yang, S.-J. Wu, Electrochim. Acta 134 (2014) 249–257.
[78] P. Carneiro, J. Loureiro, C. Delerue-Matos, S. Morais, M. do Carmo Pereira, Sens. Actuators B Chem. 239 (2017) 157–165.
[79] G. Zhao, Y. Wang, X. Li, Q. Yue, X. Dong, B. Du, W. Cao, Q. Wei, Anal. Chem. 91 (2019) 1989–1996.
[80] M. Ammar, C. Smadja, L. Giang Thi Phuong, M. Azzouz, J. Vigneron, A. Etcheberry, M. Taverna, E. Dufour-Gergam, Biosens. Bioelectron. 40 (2013) 329–335.
[81] P. Gagni, L. Sola, M. Cretich, M. Chiari, Biosens. Bioelectron. 47 (2013) 490–495.
[82] T. Hu, S. Lu, C. Chen, J. Sun, X. Yang, Sens. Actuators B Chem. 243 (2017) 792–799.
[83] D.Y. Kang, J.H. Lee, B.K. Oh, J.W. Choi, Biosens. Bioelectron. 24 (2009) 1431–1436.
[84] M.K. Kang, J. Lee, A.H. Nguyen, S.J. Sim, Biosens. Bioelectron. 72 (2015) 197–204.
[85] Y.K. Lee, K.-S. Lee, W.M. Kim, Y.-S. Sohn, PLoS One 9 (2014) e98992.
[86] A. Kaushik, P. Shah, p.k. Vabbina, R. Jayant, S. Tiwari, A. Vashist, A. Yndart, M. Nair, A Label-free Electrochemical Immunosensor for Beta-Amyloid Detection, (2016).
[87] W.A. El-Said, K. Abd El-Hameed, N. Abo El-Maali, H.G. Sayyed, Electroanalysis 29 (2017) 748–755.
[88] J.V. Rushworth, A. Ahmed, H.H. Griffiths, N.M. Pollock, N.M. Hooper, P.A. Millner, Biosens. Bioelectron. 56 (2014) 83–90.
[89] J. Qin, J.S. Park, D.G. Jo, M. Cho, Y. Lee, Sens. Actuators B Chem. 273 (2018) 1593–1599.
[90] L. Liu, N. Xia, M. Jiang, N. Huang, S. Guo, S. Li, S. Zhang, J. Electroanal. Chem. 754 (2015) 40–45.
[91] J. Qin, D.G. Jo, M. Cho, Y. Lee, Biosens. Bioelectron. 113 (2018) 82–87.
[92] H. Li, Y. Cao, X. Wu, Z. Ye, G. Li, Talanta 93 (2012) 358–363.
[93] H. Li, H. Xie, Y. Cao, X. Ding, Y. Yin, G. Li, Anal. Chem. 85 (2013) 1047–1052.
[94] H.-G. Jahnke, D. Krinke, D. Seidel, K. Lilienthal, S. Schmidt, R. Azendorf, M. Fischer, T. Mack, F. Striggow, H. Althaus, A. Schober, A.A. Robitzki, Biosens. Bioelectron. 88 (2017) 78–84.
[95] J.O. Esteves-Villanueva, H. Trzeciakiewicz, S. Martic, Analyst 139 (2014) 2823–2831.
[96] S.X. Wang, D. Acha, A.J. Shah, F. Hills, I. Roitt, A. Demosthenous, R.H. Bayford, Biosens. Bioelectron. 92 (2017) 482–488.
[97] N. Carlin, S. Martic-Milne, J. Electrochem. Soc. 165 (2018) G3018–G3025.
[98] B. Shui, D. Tao, J. Cheng, Y. Mei, N. Jaffrezic-Renault, Z. Guo, Analyst 143 (2018) 3549–3554.
[99] B. Derkus, P. Acar Bozkurt, M. Tulu, K.C. Emregul, C. Yucesan, E. Emregul, Biosens. Bioelectron. 89 (2017) 781–788.
[100] M. Vestergaard, K. Kerman, D.K. Kim, M.H. Ha, E. Tamiya, Talanta 74 (2008) 1038–1042.
[101] T. Thi Vu Nu, T. Hoa, E. Nam, T. Nguyen, W. Jung Yoon, S. Cho, J. Kim, K.-A. Chang, H. Ju, Blood-based Immunoassay of Tau Proteins for Early Diagnosis of Alzheimer's Disease Using Surface Plasmon Resonance Fiber Sensors, (2018).
[102] S. Kim, A.W. Wark, H.J. Lee, Anal. Chem. 88 (2016) 7793–7799.
[103] S. Lisi, S. Scarano, S. Fedeli, E. Pascale, S. Cicchi, C. Ravelet, E. Peyrin, M. Minunni, Biosens. Bioelectron. 93 (2017) 289–292.
[104] L. Dujuan, S. Scarano, S. Lisi, P. Palladino, M. Minunni, Sensors 18 (14248220) (2018) 946.
[105] L. Rivas, A. de la Escosura-Muñiz, J. Pons, A. Merkoçi, Electroanalysis 26 (2014) 1287–1294.
[106] L. Wu, H. Ji, H. Sun, C. Ding, J. Ren, X. Qu, Chem. Commun. (Cambridge, England) 52 (2016) 12080–12083.
[107] M. Medina-Sánchez, S. Miserere, E. Morales-Narváez, A. Merkoçi, Biosens. Bioelectron. 54 (2014) 279–284.
[108] Y. Liu, L.-P. Xu, S. Wang, W. Yang, Y. Wen, X. Zhang, Biosens. Bioelectron. 71 (2015) 396–400.

[109] A. Mars, M. Hamami, L. Bechnak, D. Patra, N. Raouafi, Anal. Chim. Acta 1036 (2018) 141–146.
[110] X.R. Cheng, B.Y.H. Hau, T. Endo, K. Kerman, Biosens. Bioelectron. 53 (2014) 513–518.
[111] X. Ren, J. Yan, D. Wu, Q. Wei, Y. Wan, ACS Sens. 2 (2017) 1267–1271.
[112] L. Liu, F. Zhao, F. Ma, L. Zhang, S. Yang, N. Xia, Biosens. Bioelectron. 49 (2013) 231–235.
[113] L. Liu, Q. He, F. Zhao, N. Xia, H. Liu, S. Li, R. Liu, H. Zhang, Biosens. Bioelectron. 51 (2014) 208–212.
[114] Y. Yu, X. Sun, D. Tang, C. Li, L. Zhang, D. Nie, X. Yin, G. Shi, Biosens. Bioelectron. 68 (2015) 115–121.
[115] S. Prabhulkar, R. Piatyszek, J.R. Cirrito, Z.Z. Wu, C.Z. Li, J. Neurochem. 122 (2012) 374–381.
[116] T.C. Liu, Y.C. Lee, C.Y. Ko, R.S. Liu, C.C. Ke, Y.C. Lo, P.S. Hong, C.Y. Chu, C.W. Chang, P.W. Wu, Y.Y. Chen, S.Y. Chen, Theranostics 8 (2018) 4210–4225.
[117] N. Xia, L. Liu, M.G. Harrington, J. Wang, F. Zhou, Anal. Chem. 82 (2010) 10151–10157.
[118] T. Hu, C. Chen, G. Huang, X. Yang, Sens. Actuators B Chem. 234 (2016) 63–69.
[119] H. Kim, J.U. Lee, S. Song, S. Kim, S.J. Sim, Biosens. Bioelectron. 101 (2018) 96–102.
[120] A. de la Escosura-Muñiz, Z. Plichta, D. Horák, A. Merkoçi, Biosens. Bioelectron. 67 (2015) 162–169.
[121] R.-a. Doong, P.-S. Lee, K. Anitha, Biosens. Bioelectron. 25 (2010) 2464–2469.
[122] N. Elahi, M. Kamali, M.H. Baghersad, Talanta 184 (2018) 537–556.
[123] A. Nag, A. Mitra, S.C. Mukhopadhyay, Sens. Actuators A Phys. 270 (2018) 177–194.
[124] M. Pumera, Mater. Today 14 (2011) 308–315.
[125] M. Pumera, A. Ambrosi, A. Bonanni, E.L.K. Chng, H.L. Poh, Trac. Trends Anal. Chem. 29 (2010) 954–965.
[126] K. Tadyszak, J.K. Wychowaniec, J. Litowczenko, Nanomaterials 8 (2018) 944.
[127] M. Pumera, Chem. Eur J. 15 (2009) 4970–4978.
[128] G.A. Rivas, M.C. Rodríguez, M.D. Rubianes, F.A. Gutierrez, M. Eguílaz, P.R. Dalmasso, E.N. Primo, C. Tettamanti, M.L. Ramírez, A. Montemerlo, P. Gallay, C. Parrado, Appl. Mater. Today 9 (2017) 566–588.
[129] H. Yoon, Nanomaterials 3 (2013) 524.
[130] C.S. Park, C. Lee, O.S. Kwon, Polymers 8 (2016) 249.
[131] S. Lee, E. Silajdžić, H. Yang, M. Björkqvist, S. Kim, O.C. Jeong, O. Hansson, T. Laurell, Microchim Acta 181 (2014) 1143–1149.
[132] L. Zhu, Z. Zhao, P. Cheng, Z. He, Z. Cheng, J. Peng, H. Wang, C. Wang, Y. Yang, Z. Hu, Adv. Mater. 29 (2017) 1700057.
[133] J. Qin, M. Cho, Y. Lee, ACS Appl. Mater. Interfaces 11 (2019) 11743–11748.
[134] T. Sunderland, G. Linker, N. Mirza, et al., J. Am. Med. Assoc. : J. Am. Med. Assoc. 289 (2003) 2094–2103.
[135] H.N. Chan, D. Xu, S.L. Ho, D. He, M.S. Wong, H.W. Li, Theranostics 9 (2019) 2939–2949.
[136] Z. Yin, S. Wang, B. Shen, C. Deng, Q. Tu, Y. Jin, L. Shen, B. Jiao, J. Xiang, Anal. Chem. 91 (2019) 3539–3545.
[137] S. Kim, J.W. Park, A.W. Wark, S.H. Jhung, H.J. Lee, Anal. Chem. 89 (2017) 12562–12568.
[138] Z. Zou, H. Yang, Q. Yan, P. Qi, Z. Qing, J. Zheng, X. Xu, L. Zhang, F. Feng, R. Yang, Chem. Commun. 55 (2019) 6433–6436.